Trees, Forests and People 18 (2024) 100657

Contents lists available at ScienceDirect

Trees, Forests and People

journal homepage: www.sciencedirect.com/journal/trees-forests-and-people

Assessment of climatic influences on net primary productivity along elevation gradients in temperate ecoregions

Kaleem Mehmood [a,b,c,1], Shoaib Ahmad Anees [d,*,1], Akhtar Rehman [e], Nazir Ur Rehman [f], Sultan Muhammad [c], Fahad Shahzad [g], Qijing Liu [a,b], Sulaiman Ali Alharbi [h], Saleh Alfarraj [i], Mohammad Javed Ansari [j], Waseem Razzaq Khan [k,l,m,*]

[a] College of Forestry, Beijing Forestry University, Beijing 100083, China
[b] Key Laboratory for Silviculture and Conservation of Ministry of Education, Beijing Forestry University, Beijing 100083, PR China
[c] Institute of Forest Science, University of Swat, Main Campus Charbagh, Swat 19120, Pakistan
[d] Department of Forestry, The University of Agriculture, Dera Ismail Khan 29050, Pakistan
[e] School of Architecture and Urban Planning, Shenzhen University China, 3688 Nanhai Blvd, Nanshan, Shenzhen 518060, Guangdong Province, China
[f] Department of Geology, Khushal khan Khattak University Karak, Pakistan
[g] Precision Forestry Key Laboratory of Beijing, Beijing Forestry University, Beijing 100083, China
[h] Department of Botany and Microbiology, College of Science, King Saud University, Riyadh 11451, Saudi Arabia
[i] Zoology Department, College of Science, King Saud University, Riyadh 11451, Saudi Arabia
[j] Department of Botany, Hindu College Moradabad (Mahatma Jyotiba Phule Rohilkhand University Bareilly, 244001, India
[k] Department of Forestry Science and Biodiversity, Faculty of Forestry and Environment, Universiti Putra Malaysia, Serdang 43400, Malaysia
[l] Advanced Master in Sustainable Blue Economy, National Institute of Oceanography and Applied Geophysics - OGS, University of Trieste, Trieste 34127, Italy
[m] Institut Ekosains Borneo (IEB), Universiti Putra Malaysia, Bintulu Campus, Sarawak 97008, Malaysia

ARTICLE INFO

KeyWords:
Net Primary Productivity
Elevation Gradient
Climatic Variables
Eddy Covariance-Light Use Efficiency (EC-LUE) Model
Human Impact on Ecosystems
Ecological Modeling

ABSTRACT

Elevation gradients significantly influence net primary productivity (NPP), but the relationship between elevation, climate variables, and vegetation productivity remains underexplored, particularly in diverse ecological zones. This study quantifies the impact of elevation and climatic variables on NPP in northern Pakistan, hypothesizing that elevation modulates NPP through its influence on temperature and precipitation patterns. Using remote sensing data (MODIS ERA5) and advanced ecological models like the Eddy Covariance-Light Use Efficiency (EC-LUE) model and the Thornthwaite Memorial Model (TMM), we analyzed Gross Primary Productivity (GPP) dynamics across various vegetation types and elevations from 2001 to 2023. Our findings show a mean annual NPP of 323.46 g C m-2 a-1, with an annual increase of 5.73 g C m-2 a-1. Significant elevation-dependent variations were observed, especially in mid-elevation zones (401 to 1600 meters), where NPP increased at a rate of 0.174 g C m-2 a-1 per meter ($R^2 = 0.808$, $p < 0.01$). In contrast, higher elevations (2800-5200 meters) exhibited a decline in NPP, decreasing by -0.171 g C m-2 a-1 per meter ($R^2 = 0.905$, $p < 0.001$). Temperature and precipitation were key drivers, with precipitation positively correlating with NPP across all vegetation types, particularly in Evergreen Needleleaf and Broadleaf Trees. The EC-LUE model's GPP estimates closely matched MODIS data ($R^2 = 0.82$), demonstrating the model's reliability. These findings highlight the critical role of elevation and climatic factors in vegetation productivity and underscore the need for targeted ecological management and conservation strategies. The insights from this research are vital for global climate adaptation policies and sustainable development goals, contributing to ecological resilience and carbon sequestration efforts worldwide.

1. Introduction

NPP is an important metric to determine the rate at which plants capture carbon, considering respiratory losses (Cui et al., 2023; Qiu et al., 2018; B. Zhou et al., 2022). NPP dramatically influences the health and carbon dynamics of forested ecosystems (Lyu et al., 2023; Wani

* Corresponding authors.
E-mail addresses: anees.shoaib@gmail.com (S.A. Anees), khanwaseem@upm.edu.my (W.R. Khan).
[1] These authors contributed equally to this work.

https://doi.org/10.1016/j.tfp.2024.100657

Available online 20 August 2024

et al., 2023; Haider et al., 2017; Jallat et al., 2021). Ecological resilience and adaptability to environmental changes in temperate forests are indicated by NPP, which reflects forest growth and health (Anees et al., 2022a; Du et al., 2024; Xue et al., 2023). Elevation gradients have a tremendous impact on NPP through altering the microclimatic conditions, like temperature and moisture availability (Chen and Zhang, 2023; He et al., 2022). These conditions in turn impact the photosynthetic abilities and growth rates of plant species (Anees et al., 2022b; Aslam et al., 2022; Huang et al., 2024). To understand the forest vegetation productivity leads to extensive insights of ecosystem functions, biodiversity assessment, and effective natural resource management (Anees et al., 2022b; Akram et al., 2022; Andreevich et al., 2020; Pan et al., 2023; Mehmood et al., 2024a). The temperate regions of Pakistan are significant due to their diverse vegetation types and unique climatic gradients (Mehmood et al., 2024d), offering an ideal setting to study how elevation and climate variables impact NPP. Understanding these dynamics is crucial for developing effective conservation strategies and sustainable forest management practices in these ecologically rich yet vulnerable areas (Anees et al., 2024a; Mehmood et al., 2024b; Muhammad et al., 2023). There are several ways through which productivity indices can be measured, and is largely dependent on the observational scale, data type's availability, and the specific ecological problems (M. Liu et al., 2023; Anees et al., 2024b; J. Wang et al., 2023; Anees et al., 2024a).

In forest ecosystems, the most accurate methods for assessing productivity are achieved through direct measurements. These direct methods include biomass harvesting and ecological plot monitoring. Biomass harvesting entails collecting all biomass within a designated area, drying it to a constant weight, and then weighing it to determine the accumulated biomass over a specified period (Luo et al., 2024; Anees et al., 2024a; Black et al., 2023; Quinkenstein et al., 2018). Ecological plot monitoring involves the long-term observation of specific research plots to track changes in tree diameter, height, and species composition (Allen et al., 2023; Idoate-Lacasia et al., 2024; Martin-Benito et al., 2022). These observations, coupled with established allometric equations, allow for the estimation of biomass (Luo et al., 2024; Anees et al., 2024a) and productivity (Li et al., 2023; Martin-Benito et al., 2022). Additionally, the integration of field-based surveys with LiDAR technology enables the generation of 3D images of forest canopies, which are instrumental in estimating forest biomass and productivity (Sabzchi-Dehkharghani et al., 2024). Beyond direct measurements, ecological models play a pivotal role in forest productivity assessment. These models incorporate a range of biotic and abiotic variables and are derived from various data sources (Patacca et al., 2023; C. Wang et al., 2023). Process-based models, such as Biome-BGC and 3-PG, simulate critical processes including photosynthesis, respiration, and nutrient cycling based on plant physiology and environmental interactions. These models are essential for predicting the effects of climate change, shifts in species composition, and forest management practices on forest productivity (Qin et al., 2023; Yu et al., 2024).

Recent advancements in remote sensing and ecological modeling, such as satellite sensors, aerial photographs, and Light Detection and Ranging (LIDAR), have become powerful tools for estimating forest productivity at regional and global scales (Massey et al., 2023; Mazlan et al., 2023). Such methodologies measure vegetative characteristics closely correlated to productivity levels and have significantly improved our ability to estimate and monitor NPP with high spatial and temporal resolution (Yin et al., 2023; Zhang et al., 2023). For instance, the application of Sentinel-1 SAR data, combined with nonparametric regression methods like Relevance Vector Regression (RVR), has demonstrated high accuracy in estimating rice crop height and biomass, achieving correlation coefficients (R^2) as high as 0.92 (Sharifi & Hosseingholizadeh, 2020). Similarly, hyperspectral image analysis has been enhanced through deep networks embedded in genetic algorithms (CNNeGA), significantly reducing data redundancy while maintaining accuracy levels between 90% and 99% (Esmaeili et al., 2023). These advancements parallel the role of the Moderate Resolution Imaging Spectroradiometer (MODIS) sensors on NASA's Terra and Aqua satellites in evaluating vegetation health and productivity (Karmakar et al., 2024; Wongnakae et al., 2023). The MCD18C2 Version 6.1 PAR data product provides more accurate estimates with improved temporal resolution through advanced algorithms (He et al., 2023). Furthermore, the integration of 3D-convolutional neural networks and attention convolutional LSTM approaches has proven effective in crop yield prediction, particularly in soybean yield prediction in the USA, with mean absolute error (MAE) values as low as 4.3 (Nejad et al., 2022). The EC-LUE model leverages light use efficiency principles to estimate GPP using absorbed PAR and environmental stress factors, including temperature and moisture, converting remote sensing data into useful ecological applications that support management and conservation restoration (Cheng et al., 2023; Lv et al., 2023). The NDVI and PAR indices have been extensively utilized in monitoring plant growth conditions and production rates over extensive areas. The satellite-based NDVI continues to be an invaluable tool for assessing photosynthetic activity and productivity (X. Chen et al., 2023; Mehmood et al., 2024b).

Elevation gradients have a unique and profound impact of biological productivity as they inherently create different climatic conditions over a short geographic range. These differences in the climatic variables such as temperature and precipitation result in defined biotic zones that feature discrete productivity profiles (An et al., 2024; Ramirez, 2016). It is found that lower elevations generally support higher NPP due to warmer temperatures and greater moisture availability (Schwartz et al., 2015; Tao et al., 2022). In contrast, higher elevations experience reduced NPP due to lower atmospheric pressure and the physiological limitations of cooler temperatures (Wei et al., 2023; Xu et al., 2024). Moreover, multiple studies in different regions of the globe with distinct climates and landscapes have proven the high variability of NPP with elevation. Thus, in a Mediterranean beech forest in Greece, ANPP was inversely associated with elevation due to water shortage and strong winds on high altitudes (Zianis and Mencuccini, 2005). Contrary to common trends observed in other regions, research in the Central Himalayan forests has shown that high NPP is not necessarily related to elevation. Despite the typical decline in productivity with increasing elevation due to temperature and other climatic factors, these studies indicate that high productivity can occur at any elevation, both in lowlands and highlands. This finding challenges the conventional understanding and highlights the unique ecological dynamics of the Central Himalayas (Rana et al., 1989). However, in tropical environments, such as Mauna Loa, Hawai'i, the situation is more complicated, and NPP depends on regional variation in ecosystem development, with high NPP near sea level (Raich et al., 1997). Our study addresses a substantial research gap as it dives deeper into the nature of elevation effects on NPP. This issue has yet to be discussed in our climatic settings, i.e., temperate regions of Pakistan. Additionally, the present research is distinguished by combining a variety of high-quality remote sensing information, climate predicting models, and ground truth data that enriches the information about productivity dynamics. Moreover, advanced ecological modelling, specifically EC-LUE and TMM, predict productivity and help identify ecological responses to climatic variations, significantly enriching the novel technique. The primary objective of this study is to quantify Net Primary Productivity (NPP) and assess its variability along an elevation gradient within the study area. Specifically, we aim to: 1) Analyze how NPP fluctuates across different vegetation types, from subtropical to temperate and alpine zones. 2) Evaluate the impact of key climatic variables, particularly temperature and precipitation, on NPP using advanced remote sensing data. 3) Implement and assess the performance of ecological models, including the EC-LUE model, in estimating vegetation productivity, facilitated by the integration of MODIS and ERA5 products.

2. Methods and materials

2.1. Study area

The study area is located within the coordinates 34.9526° N, 72.3311° E, and covers selected districts across Khyber Pakhtunkhwa (KPK), Gilgit Baltistan (GB), and Azad Jammu and Kashmir (AJK) in Pakistan. The districts included in the study are: KPK: Abbottabad, Bajaur, Kohistan Upper, Kolai Palas Kohistan, Kurram, Lower Dir, Mansehra, Swat, Tor Ghar, Upper Dir, Batagram, Kohistan Lower, Shangla, Khyber, Mohmand, North Waziristan, Orakzai, and South Waziristan. GB: Darel and Tangir. AJK: Neelum, Bagh, Hattian Bala, Haveli, and Muzaffarabad. These areas are chosen due to their diverse vegetation types, from subtropical in the southern parts to temperate and alpine regions in the north. They provide a wide elevation range from approximately 290 to 5550 meters (Ahmed, 2011; Sayed and González, 2014) (Fig. 1).

The presence of these specific regions is crucial for examining the distribution and impact on NPP across a gradient of elevation, especially regarding climate variables such as temperature and precipitation (Zafar et al., 2021). The research utilizes the unique ecological variations present in these areas and denser plant growth in northern districts like Swat and Mansehra compared to the subtropical conditions in South Waziristan and Orakzai. This variation is essential for studying how different environmental factors affect vegetation dynamics, offering important insights for managing ecology and conservation efforts in these high-altitude zones (Mehmood et al., 2024c).

2.2. Data retrieval and initial processing

2.2.1. Datasets for estimating GPP, NPP, and PNPP

We utilized a collection of high-quality datasets with high resolution to estimate GPP, NPP, and PNPP. Table 1 provides a detailed overview of the data sources we selected for their capacity to offer precise temporal and spatial information on the factors that impact terrestrial ecosystems. The photosynthetically active radiation (PAR) data from the MCD18C2 Version 6.1 PAR data product sourced from the MODIS Terra and Aqua satellites (Wang et al., 2020). This product offers a more enhanced temporal resolution than the previously used products (Xu et al., 2024; Yuan et al., 2007). The MCD18C2 product utilizes a refined algorithm for varying aerosol loadings, cloud conditions, and illumination/viewing geometries. This makes it a more dynamic and precise data source for assessing PAR. Each satellite pass offers instantaneous PAR measurements, and the compiled data delivers comprehensive coverage with a spatial resolution of 0.05° (Luo et al., 2023). These features make it suitable for accurate and detailed analysis, aligning with the needs of our study. The NDVI data, essential for assessing vegetation health and productivity, was sourced from the MODIS (MOD13A1 V6.1) product available through NOAA-AVHRR. The dataset is processed using Google Earth Engine (GEE) to ensure high-quality, atmospheric-corrected surface reflectance measurements, minimizing errors from clouds, aerosols, and other atmospheric disturbances (http://earthengine.google.com/). The NDVI data was compiled using the Maximum Value Composite (MVC) method to optimize the accuracy of vegetation dynamics monitoring (Fan et al., 2020; Mehmood et al., 2024b). In order to better understand how climate affects vegetation productivity (Gallardo et al., 2024; Rita et al., 2020), we used data on temperature and dew point temperature from ERA5, the most up-to-date climate reanalysis by the European Centre for Medium-Range Weather Forecasts (ECMWF) (Muñoz-Sabater et al., 2021a; Y.-R. Wang et al., 2022). ERA5 provides monthly data on a wide range of atmospheric variables at a higher spatial resolution of 0.1° better than ERA-LAND, which enables a more detailed and dynamic analysis of the impacts of temperature on ecological productivity (Gomis-Cebolla et al., 2023).

To integrate MODIS and ERA5 data effectively, we employed a resampling technique to reconcile their differing spatial resolutions. Specifically, we upscaled the MODIS data with a spatial resolution of 0.05° to match the 0.1° resolution of the ERA5 data using bilinear

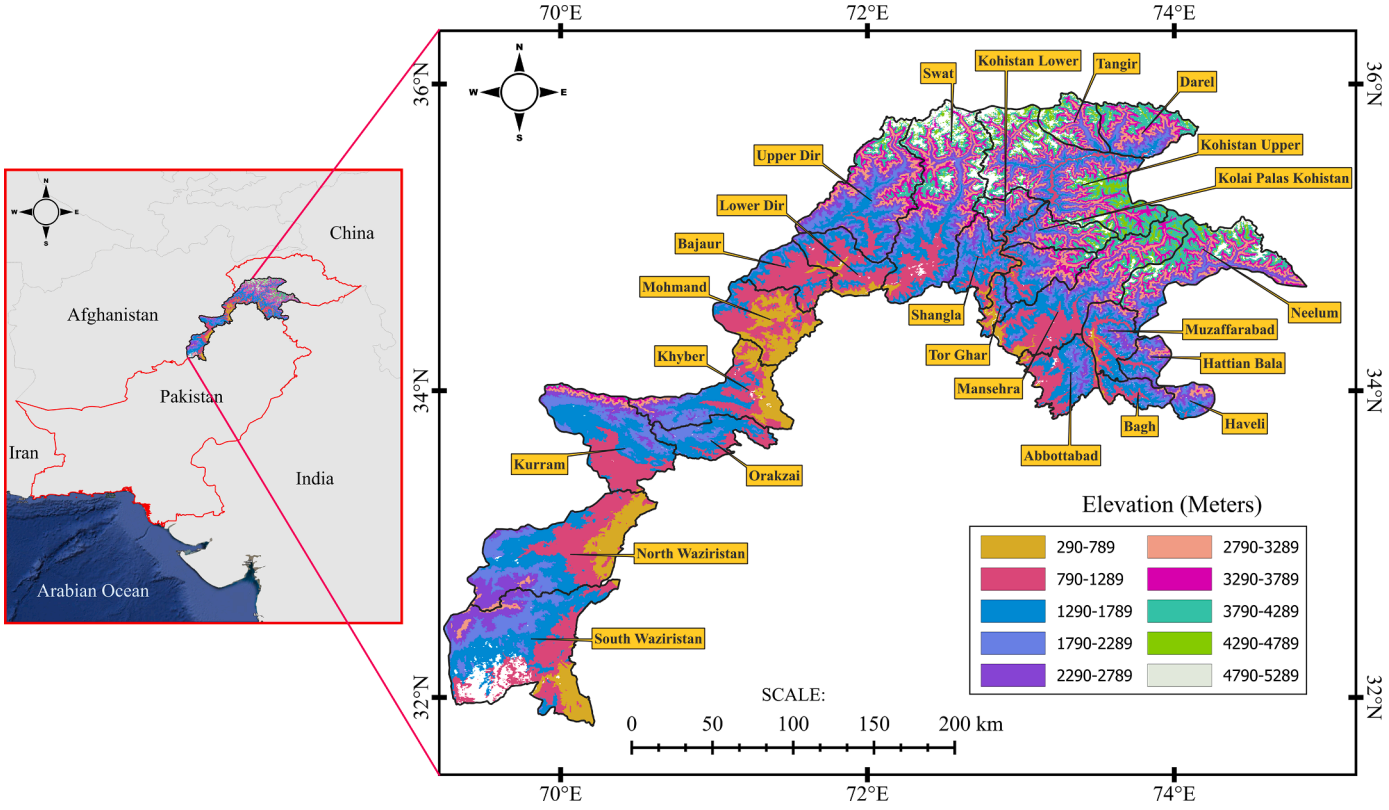

Fig. 1. Geographical and Elevation Characteristics of the Study Area.

Table 1
Data sources and applications for GPP, NPP, and PNPP calculation.

Data Type	Source	Spatial Resolution	Temporal Resolution	Description	Reference
PAR	MODIS	0.05°	3-hour intervals	MCD18C2 Version 6.1	(Z. Wang et al., 2022)
NDVI	MODIS	500m	16 days	MOD13A1 V6.1	(Sa and Fan, 2023) (Mehmood et al., 2024b)
Temperature and Dew Point	ERA5	0.1°	Monthly	ECMWF	(Muñoz Sabater, 2019; Muñoz-Sabater et al.,2021b; Sobrino and Jiménez-Muñoz, 2014)
Precipitation	CHIRPS	0.05°	Pentad	High-resolution estimates combining satellite imagery with in-situ data.	(de Sousa et al., 2020; Mashao et al., 2023)
Topography (DEM)	ALOS World 3D - 30m (AW3D30)	30m	Static	High-resolution elevation data critical for assessing terrain influences on ecological productivity.	(Bakiev et al., 2022; Takaku et al., 2020)
Land Cover	MODIS Land Cover Type	500m	Annually	(MCD12Q1) V6.1	(Zhou et al., 2020)
Carbon Use Efficiency (CUE)	MODIS Terra GPP & NPP	500m	Annually	(MOD17A3HGF)	(Manzoni et al., 2012; Yang et al., 2023)

interpolation. This method ensures that the finer spatial details of the MODIS data are retained while aligning with the coarser grid of the ERA5 dataset (Muñoz-Sabater et al., 2021). Additionally, any potential discrepancies due to temporal resolution differences were addressed by averaging the higher frequency MODIS data to match the monthly resolution of ERA5. This approach minimizes potential inaccuracies and allows for a seamless integration of the datasets, providing a robust foundation for our analysis of GPP, NPP, and PNPP (Wang et al., 2023).

We evaluated the impact of water availability on plant productivity using the CHIRPS dataset for precipitation data. CHIRPS offers high-resolution pentad precipitation estimates, with a spatial resolution of around 0.05 degrees, by combining satellite imagery with in-situ station data to improve measurement reliability, particularly in under-monitored regions (de Sousa et al., 2020; Ren et al., 2023). This dataset has comprehensive spatial and detailed temporal coverage, which provides accurate hydrological inputs, leading to improved estimation of GPP across various ecological settings in the EC-LUE model (Vargas Godoy and Markonis, 2023). To ensure an accurate calculation of the influence of elevation on NPP in our study, we made use of the ALOS Global Digital Surface Model, "ALOS World 3D - 30m (AW3D30)" as our primary source for topographical data (JAXA, 2019). This dataset is crucial for detailed ecological modeling, providing high-resolution elevation data with 30-meter accuracy (Bakiev et al., 2022; Takaku et al., 2020). The ALOS DEM's enhanced resolution enables us to identify the elevation gradients precisely, which is essential to a more nuanced analysis of how varying altitudinal conditions affect NPP across the study area. The MODIS Land Cover Type (MCD12Q1) Version 6.1 data product from the USGS LP DAAC was used in this research to obtain land cover data (https://lpdaac.usgs.gov/). It provides annual global land cover classifications obtained from reflectance data collected from MODIS sensors (Terra and Aqua satellites) through supervised classification. Our study utilized the Annual Plant Functional Types (APFTC) classification scheme from this dataset. This classification scheme offers a spatial resolution of 500 meters and is updated annually (Naghdizadegan Jahromi et al., 2021; Zhao et al., 2020). Our detailed analysis concentrated on six vegetational classes selected from the eleven LULC classes provided. These classes include Evergreen Needleleaf Trees (ENT), Evergreen Broadleaf Trees (EBT), Deciduous Needleleaf Trees (DNT), Deciduous Broadleaf Trees (DBT), Shrubs (S), and Grass (G). This set of advanced datasets is available to estimate GPP, NPP, and PNPP comprehensively. These datasets incorporate improved spatial and temporal resolutions that accurately capture dynamic ecological processes. By using this data framework, we can analyze the productivity and ecological dynamics more effectively, which is vital for understanding complex ecosystem interactions.

2.2.3. Data selection for estimating CUE

Carbon Use Efficiency (CUE) is a significant ecological measure that is utilized to calculate the effectiveness of plants in converting absorbed carbon to stored biomass, which is represented by NPP through the process of GPP. It can be expressed as the ratio of NPP and GPP (Eq. 1) (Hilker et al., 2008; Ingle et al., 2023; Liao et al., 2023; Lv et al., 2023).

$$CUE = \frac{GPP}{NPP} \tag{1}$$

The MODIS Terra dataset (MOD17A3HGF) was preferred as it involves a comprehensive range of climatic components including atmospheric CO_2 levels, solar radiation, and Vapor Pressure Deficit (VPD) for the calculations. These variables are essential to accurately capture the spatial, seasonal, and annual variations in GPP, particularly in showing yearly fluctuations (Running and Zhao, 2019). We have also utilized the same MODIS dataset that provides ANPP values at a 500 m resolution. The ANPP values were calculated by summing all 8-day net photosynthesis (PSN) data from the specified year. The difference between GPP and maintenance respiration (MR) determines PSN, which is critical in accurately calculating the annual carbon accumulation (Teubner et al., 2019). The utilization of MODIS data, especially for GPP, is advantageous due to its sophisticated algorithmic approach that efficiently integrates crucial environmental impacts, providing a more precise and detailed representation of GPP across varied landscapes (Huang et al., 2021; Y. Li et al., 2021; Liu et al., 2014). This comprehensive approach enhances the accuracy and reliability of our carbon flux analysis, making MODIS an optimal choice for detailed studies of ecosystem carbon dynamics.

2.3. Methodology

2.3.1. Estimating GPP and ANPP in temperate ecosystems of Pakistan using the EC-LUE model

We applied the EC-LUE model to estimate GPP in temperate environments in Pakistan. This model assumes a linear relationship between FPAR and NDVI and posits that actual light use efficiency is influenced by temperature and soil moisture, with the limiting factor being more influential (J. Zhang et al., 2021; Zhang et al., 2015). The model's GPP estimates were validated against daily measurements from 28 flux towers, accounting for up to 85% of observed GPP variations. Compared with MODIS-derived GPP, the EC-LUE model demonstrated superior alignment, confirming its effectiveness in capturing primary productivity dynamics (Xu et al., 2024; Yuan et al., 2007). The EC-LUE model formula utilized in this study to calculate Gross Primary Productivity (GPP) is expressed as (Eq. 2):

$$GPP = \epsilon max \times PAR \times FPAR \times \min(T_s, W_s) \tag{2}$$

Where ϵ_{max} (2.25 g C/MJ) represents the maximum light use efficiency, and FPAR is derived from NDVI (Junttila et al., 2023; Milesi and Kukunuri, 2022; Yuan et al., 2015). The terms T_s and W_s represent temperature and water stress limits, respectively, following the "minimum factor rule," which states that the most restrictive environmental factor constrains GPP (Xi and Yuan, 2023; W. Zhang et al., 2024). Based on established research, the mathematical equations for estimating FPAR, Ts, and Ws are given as (Eq 3-5):

$$FPAR = a \times NDVI \times b \quad (3)$$

$$T_s = \frac{(T - T_{min})(T - T_{max})}{(T - T_{min})(T - T_{max}) - (T - T_{opt})} \quad (4)$$

$$W_s = \frac{VPD_o}{(VPD_o + VPD)} \quad (5)$$

In equation 3, a and b are empirical coefficients with respective values of 1.24 and -0.168. whereas T_{min}, T_{max}, and T_{opt} are the minimum, maximum, and optimal temperatures for photosynthesis, set to 0°C, 40°C, and 21°C, respectively (Ding et al., 2023; Wiltshire et al., 2021). The vapor pressure deficit (VPD) is calculated using saturated and actual vapor pressure, adjusted for air pressure using the enhancement factor f_w (Yuan et al., 2010; Gan et al., 2018). For a detailed breakdown of the VPD calculation and the underlying equations (Appendix A).

ANPP was derived using CUE, calculated as the ratio of NPP to GPP

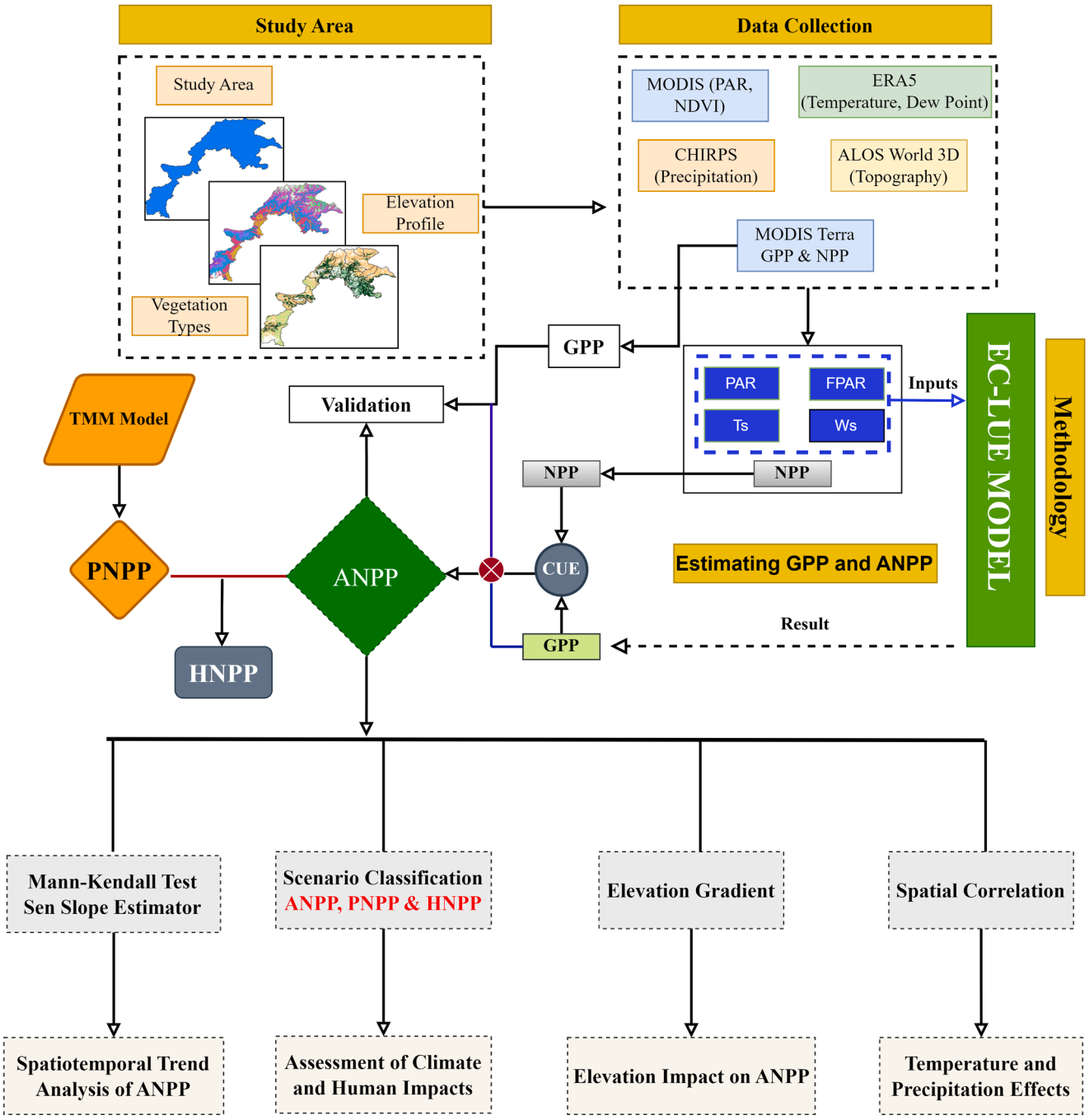

Fig. 2. Schematic diagram illustrating the overall methodology for assessing the impacts of climate and human factors on NPP using remote sensing and statistical techniques.

(Eq 6). Although traditionally assumed constant at 0.5, recent research indicates CUE can vary due to environmental and ecological factors (da Costa et al., 2014; Kunert and Aparecido, 2024; S. Chen et al., 2023; Nouvellon et al., 2000; Ukkola et al., 2021). We computed CUE at a pixel scale for more accurate ecosystem interaction representation, as depicted in the schematic diagram (Fig. 2).

$$ANPP = GPP \times CUE \tag{6}$$

2.3.2. Deriving Estimates for PNPP and HNPP

We utilized the Thornthwaite Memorial Model (TMM), an advanced version of the Miami Model, to estimate Potential Net Primary Productivity (PNPP) by incorporating precise climate data, particularly temperature and precipitation, to assess annual actual evapotranspiration (Teng et al., 2023; Tu et al., 2023). The TMM's effectiveness and reliability in ecological research are well-documented (Bi et al., 2023; Lu et al., 2023).

PNPP is determined by the equation:

$$PNPP = C \times (1 - exp(-d \times (v - 20))) \tag{7}$$

In this formula, v, which denotes the annual actual evapotranspiration (mm), is calculated from:

$$v = \frac{a \times r}{\sqrt{1 + \left(1 + \frac{a \times r}{L}\right)^2}} \tag{8}$$

And L, which is the equation for annual average evapotranspiration (mm), is formulated as:

$$L = C + b \times t + c \times t^3 \tag{9}$$

In these equations, CCC (3000 mm) represents maximum potential evapotranspiration under ideal conditions, d (0.0009695) modulates the influence of evapotranspiration on PNPP, a (1.05) adjusts for precipitation's impact, and b (25) and ccc (0.05) represent the linear and cubic coefficients for temperature's effect on evapotranspiration. Here, r is annual total precipitation (mm), and t is the annual mean temperature (°C). To enhance the accuracy of PNPP estimates, additional variables such as wind speed and solar radiation from the ERA5 dataset were included, particularly for regions with significant climatic variations (Gao et al., 2008; C. Li et al., 2021).

HNPP (Human-impacted Net Primary Productivity) is calculated by subtracting ANPP (Annual Net Primary Productivity) from PNPP.

$$HNPP = PNPP - ANPP \tag{10}$$

This metric quantifies the influence of human actions, including urbanization and agriculture, on vegetation productivity.

2.4. Trend analysis

2.4.1. Sen slope

The Sen's Slope Estimator is an essential method for analyzing changes in environmental and climatological factors over time (Liu et al., 2020; Mehmood et al., 2024b; Society et al., 2021; Mehmood et al., 2024d). This technique helps to identify trends in real-world environmental data, which can be affected by irregular fluctuations and outliers. To use this technique, data is first organized into ordered pairs (xi, yi), where x_i represents time intervals, and y_i represents the corresponding values of the ANPP.

The analysis involves calculating the slopes S_{ij} between all possible pairs of data points in the series while ensuring that $i < j$. The slope for each pair is determined using a specific formula.

$$S_{ij} = \frac{y_j - y_i}{x_j - x_i} \; where \; j > i \tag{16}$$

This formula calculates the rate of change between every pair, thus capturing a comprehensive gradient that reflects the overall trend over time. After determining all potential slopes, the median of these values is calculated. This median slope is significantly vital against outliers, providing a more reliable measure of central tendency than the mean, which is crucial in datasets with potential anomalies. This methodology not only explains the rate of change of ANPP but also helps in understanding how various environmental factors might be influencing these changes, providing a solid foundation for further ecological analysis and decision-making (Mehmood et al., 2024d).

2.4.2. Mann Kendal

The Mann-Kendall trend test is a reliable method that examines the existence of a monotonic trend in sequential data sets, such as ANPP (Frimpong et al., 2022; Mehmood et al., 2024b; Khaniya et al., 2020; Mehmood et al., 2024d). This non-parametric test eliminates the need for data to conform to a normal distribution and is less susceptible to outliers (Verma et al., 2016). By analyzing the entire set of data points, the test computes the test statistic S by adding the signs of variances between paired observations (Garba and Udokpoh, 2023; Mehmood et al., 2024d).

$$S = \sum_{i=1}^{n-1} \sum_{j=i+1}^{n} sgn\left(y_i - y_j\right) \tag{17}$$

Here, yi and yj represent data values at times i and j (where $j > i$), and the function sign(x) is defined as follows (Eq. 18): +1 if $x > 0$, 0 if $x = 0$, and -1 if $x < 0$ (Ali et al., 2019).

$$sgn(x_j - x_k) = \begin{cases} +1 \; when \; (x_j - x_k) > 0 \\ 0 \quad when \; (x_j - x_k) = 0 \\ -1 \; when \; (x_j - x_k) < 0 \end{cases} \tag{18}$$

The S variance is used to standardize the test statistic under the null hypothesis of no trend, as it follows a normal distribution (Eq). The test is robustly used to assess whether the trend has declined or increased over time, as it does not allow for violations of ecological trends due to excessive noise or any underlying data distribution (Garba and Udokpoh, 2023).

$$Var(S) = \frac{n(n-1)(2n+5) - \sum_{p=1}^{q} tp \; (tp-1)(2tp+5)}{18} \tag{19}$$

Here, n represents the total number of data points. tp denotes the number of tied groups in the $p - th$ group, and q represents the total number of tied groups

After calculating S and Var(S), we can determine the trend significance using the standardized test statistic Z, especially if $n > 10$, which is typical in environmental datasets. The formula for calculating Z is given by (Eq. 20).

$$Z = \begin{cases} \frac{s-1}{\sqrt{var\ (s)}} & when \; S > 0 \\ 0 & when \; S = 0 \\ \frac{s+1}{\sqrt{var\ (s)}} & when \; S < 0 \end{cases} \tag{20}$$

To determine the presence of a trend, a hypothesis test is conducted by comparing the Z value to a standard normal distribution. A positive Z value indicates an upward trend, whereas a negative value suggests a downward trend (Mehmood et al., 2024b; Nyikadzino et al., 2020; Mehmood et al., 2024d). The null hypothesis posits that no trend exists, and its acceptance or rejection is contingent upon the level of significance, which is commonly established at $p < 0.05$ (Mehmood et al., 2024d).

2.4.3. Assessing Ecological Productivity Trends and Scenario Classification

During the research period, ANPP, PNPP, and HNPP slopes provided a quantitative basis to evaluate ecological changes at the pixel level. These slopes acted as critical indicators of productivity and how climatic

factors and human activities influenced it at each location. A positive slope in ANPP indicated an overall increase in productivity, which could have been driven by favorable climatic conditions or effective human management practices that enhanced ecological health. On the other hand, a negative slope in ANPP indicated a decline in ecosystem productivity, which could have been due to adverse climatic impacts or harmful human activities that detracted from ecological stability (Huang et al., 2023; X. Zhou et al., 2022). The slopes of PNPP and HNPP provided additional insights into the specific nature of these influences. A positive slope in PNPP generally signified beneficial climate effects on productivity, whereas a negative slope often indicated harmful climatic impacts (H. Li et al., 2021). Similarly, a positive slope in HNPP indicated detrimental impacts from human activities on productivity, whereas a negative slope suggested that human interventions were contributing positively to productivity. Table 2 shows nine (09) distinct scenarios have been identified to explain the various influences on ecosystem health.

3. Results

3.1. Temporal Trends and Spatial Variability in ANPP, PNPP, and HNPP

The ANPP was 323.46 g C m^{-2} a^{-1} in the study area from 2001 to 2023, with an annual increase of 5.73 g C m^{-2} a^{-1}, indicating substantial ecological variation. The PNPP was significantly higher, averaging 534.99 g C m^{-2} a^{-1}, with an even more notable annual increase of 11.058 g C m^{-2} a^{-1}, reflecting the area's maximum potential ecological productivity (Table S1). HNPP, estimated as the difference between PNPP and ANPP, averaged 211.61 g C m^{-2} a^{-1} with an annual increase of 5.325 g C m^{-2} a^{-1} (Fig. 6). It shows a significant human impact on the natural productivity of ecosystems. Spatial patterns of ANPP encompassed a different values across various zones. The majority of the area 42.75%, displayed very low productivity, lower than 200 g C m^{-2} a^{-1}, suggesting regions heavily impacted by stress or human activities (Fig. 5a). Zones characterized by low to moderate productivity levels, ranging from 200-600 g C m^{-2} a^{-1}, covered 45.73% of the area and included regions in recovery or enduring less impact. Higher productivity zones, from 600-800 g C m^{-2} a^{-1}, accounted for 11.2%, and very high productivity zones, exceeding 800 g C m^{-2} a^{-1}, comprised just 0.25% of the entire area (Table S2), indicating that optimal functioning ecosystems were extremely minimal.

For PNPP, the distribution across different productivity classes indicates varied ecological potential. The largest portion of the landscape, 33.85%, has PNPP not more than 200 g C m^{-2} a^{-1}, highlighting significant areas that are ecologically limited. The next substantial categories include areas with PNPP ranging from 200-600 g C m^{-2} a^{-1} and 600-1200 g C m^{-2} a^{-1}, which account for 29.56% and 26.21% of the landscape, respectively, suggesting moderate ecological productivity (Fig. 5b). Areas with higher productivity, between 1200-1800 g C m^{-2} a^{-1}, represent 10.11% of the landscape, while zones with very high productivity over 1800 g C m^{-2} a^{-1} are exceptionally rare (0.27%) (Table S3). HNPP values, representing the impact of human activity, show that a significant portion of the area, 45.92%, has very low HNPP (<100 g C m^{-2} a^{-1}), which may indicate substantial reductions in ecological productivity due to human activities. The remaining areas exhibit higher HNPP values, with 53.66% of the landscape falling within the 100-900 g C m^{-2} a^{-1} range, suggesting such areas still maintain moderate to high levels of productivity despite potential anthropogenic pressures. Especially, zones with HNPP greater than 900 g C $m^{-2}a^{-1}$ are exceedingly rare, comprising only 0.42% of the area (Fig. 5c) (Table S4), highlighting the scarcity of areas with very high productivity.

In turn, it becomes clear that it is important to implement specific ecological management to address productivity-related questions based on the specific areas' challenges and potentials. While the efforts should be focused on the restoration in lagging-behind areas to increase productivity, certain areas with ample potential require serious protective measures to prevent ecological loss (Khan et al., 2020; Khan et al., 2024). The zonal analysis of ANPP across 25 districts in AJK, GB, and KPK shows substantial variability in ecosystem productivity (Fig. 5d). The mean ANPP was 385.03 g C m^{-2} a^{-1}, with a standard deviation of 183.00 g C m^{-2} $a^{-1}$and a range of 108.76 to 644.22 g C m^{-2} $a^{-1}$and a median of 435.20 g C m^{-2} a^{-1}. These results show that the districts varied significantly in ecological conditions and management practices. Approximately 25% of the districts were below 238.86 g C m^{-2} a^{-1}, reflecting low productivity zones where ecological productivity or human stress was more considerable. These districts include Tangir, Khyber, Mohmand, North Waziristan, Orakzai, and South Waziristan. In contrast, the top 25% of districts exceeded 533.37 g C m^{-2} a^{-1}, showing either a high potential for productivity or effective management practices. These districts include Bagh, Neelum Valley, Haveli, Muzaffarabad, Batagram, Kohistan Lower, and Shangla. Overall, this analysis underscores the need for the development of district-specific ecological management strategies. For instance, low productivity districts such as Tangir and Khyber would require intervention to increase productivity through restoration activities, while high productivity districts such as Bagh or Muzaffarabad would need interventions to maintain productivity through conservation.

Table 2
Scenario classification based on ANPP, PNPP, and HNPP trends.

Scenarios	S_{ANPP}	S_{PNPP}	S_{HNPP}	Driving force	Abbreviation
Climate Positive Impact	>0	>0	>0	Climate Dominant	CPD
Human Negative Impact	>0	<0	<0	Human Dominant	HNI
Mixed Climate and Human Impact	>0	>0	<0	Climate and Human	MCH
Data Inconsistency Error	>0	<0	>0	Data Error	DER
Climate Negative Impact	<0	<0	<0	Climate Dominant	CND
Human Positive Impact	<0	>0	>0	Human Dominant	HPD
Conflict Climate and Human Impact	<0	<0	>0	Climate and Human	CCH
Data Inconsistency Error	<0	>0	<0	Data Error	DEN
No Impact Scenario	0	0	0	No Dominant Force	NDF

3.2. Trend analysis

The analysis of Mann-Kendall trend for ANPP reveal a mixed trajectory of ecological changes among the districts under consideration over the study duration. Most of the study area, covering 72.44%, depicts a significant positive trend in ANPP ($p < 0.01$), indicating a considerable significant increase in vegetation's health and productivity levels. The positive changes in ANPP align significantly attributed to the Billion Trees Afforestation Project (BTAP), implemented from 2014 to increase the forest cover. The positive trend is fundamentally due to a combination of natural restoration occurring following the environmental changes, active conservation, selective afforestation through the BTAP and restoration after disturbances. However, very little of the total area, 0.11%, indicates a significant negative trend ($p<0.01$), decreasing ANPP (Fig. 7). The declining trend is critical since it signals the likely stressed blocks of the ecosystem due to environmental factors such as deforestation, urban expansion and unfavorable climate for vegetation.

In districts where the trends are significant with a p-value less than 0.05, but not as strong as at the $p<0.01$ significance level, we observe that 6.56% of the area exhibits a positive trend and 0.12% shows a negative trend. It is possible that these areas are experiencing subtler shifts in ecological conditions or management practices that influence productivity trends, either positively or negatively. Finally, areas where

increasing productivity trends are detected at the $p < 0.10$ significance level encompass 3.32% of the study area. Such areas might indicate emerging improvements in ANPP that warrant further investigation to identify the contributing factors. Lastly, areas with non-significant trends ($p>0.10$) cover 17.34% of the area, split into 14.13% showing a non-significant positive trend and 3.21% showing a non-significant negative trend. These districts may represent zones where ANPP is relatively stable, with no clear directional changes, or where variability in productivity is influenced by a mix of counteracting factors that dilute a clear trend. The stability in ANPP within these regions could be due to balanced climatic conditions and resilient vegetation types that maintain consistent productivity (Polley et al., 2013). Additionally, effective local land management practices, such as sustainable forestry and agriculture, may mitigate the impacts of climate extremes. These areas might also experience counteracting factors like periodic droughts balanced by irrigation, highlighting the need for targeted management strategies (Yin et al., 2022).

As a result, the research develops a sophisticated classification of ecological landscapes on the basis of interrelations between ANPP, PNPP, and HNPP, outlining nine unique categories that deficits various environmental dynamics and human involvement (Table 2). Dominating the study, approximately 95.91% of the area falls under CPD, signifying a substantial increase in productivity. This category underscores regions which have a positive impact on ecological well-being, playing a key part in carbon sequestration and the preservation of biodiversity. HNI though, very low and covering 0.15% of the landscape, allows for concentration of disturbances. This index is important to highlight areas where certain human activities lead to productivity declines associated with urban sprawl, deforestation, and unsustainable agriculture such categories exhibit significant adverse effects that can even overpower expected favorable climate signals. Although MCH covers only 0.36% of the area, and CCH covers another 0.098%, they demonstrate how complicated a common factor of human-made changes concord climatic conditions could be. More specifically, they reflect instances when on the surface, changes introduced by human-beings could create good conditions while large-scale adverse changes cannot be prevented. It is critical evidence for the necessity of balance between human development and environmental sustainability. Areas highlighted for DER and DEN, not exceeding 0.023% of the landscape's total output, are vital for highlighting measurement errors or inconsistencies. These errors might indicate environmental phenomena that standard models are not designed to detect or could signal wrong data entry, highlighting the need for accurate data in ecological study.

The CND affects 3.2% of the study area, illustrating a scenario where all forms of productivity decline (Fig. 8), likely due to harsh climatic conditions like drought or extreme weather events. This category is essential for identifying regions at high risk of ecological degradation, necessitating focused conservation efforts to mitigate the influences of climate change. Similarly, the HPD and No Dominant Force NDF, although relatively small in area coverage (0.18% and 0.177% respectively), highlight regions where human interventions have successfully enhanced ecological productivity or where no significant productivity changes have been detected. The scenario classification for the study area across different vegetation types primarily reveals a CPD dominance, especially in ENT and EBT, which collectively account for over 97% of the area. This serves as evidence to the climatic benefits supporting their productivity. Nevertheless, DNT and Grasslands exhibit presence of CND, highlighting vulnerabilities that could compromise the health of these ecosystems, accounting for 10.13% and 5.14% of the area, respectively. These findings suggest areas where current land management practices might be effectively supporting sustainability or where ecological conditions have remained stable despite potential pressures. These categories provide a structured, comprehensive framework that facilitates a detailed analysis of how climate dynamics, human activities, and ecological productivity are intertwined. The mapping not only highlights the varied ecological responses to different pressures but also supports the development of targeted interventions tailored to the unique challenges and opportunities within each category. This approach ensures that the interventions are both comprehensive and sustainable.

3.3. Ecological responses to altitudinal variations of ANPP

The elevation gradient of the region was divided into 100-meter distinct zones to determine the spatial heterogeneity and trends of ANPP (Fig. 9a). Each elevation range is suitable for assessing the response of ANPP to variations in altitudes. Th elevation range 0 to 400 meters showed a mild positive trend of ANPP with variation in elevation as ANPP variations with elevation increase at the rate of 0.19 g C $m^{-2}a^{-1}$ for each meter increase in elevation ($R^2 = 0.808$, $p > 0.01$). At these lower elevations, moderate temperatures, higher moisture availability, and fertile soils with adequate nutrients promote optimal photosynthetic activity and plant growth, contributing to the positive trend in ANPP. A significant strong positive trend was observed from 401 to 1600 meters with an ANPP rate of 0.174 g C $m^{-2}a^{-1}$ for each elevation meter ($R^2 = 0.808$, $p < 0.01$). There is robust increase in ANPP in this zone signifying optimality in vegetation growths in this broader elevation area. The elevation gradient ranged 1600 to 2800 showed an insignificant effect of ANPP with changes in elevation that is, ($R^2 = 0.08$, $p > 0.01$) with only slight change of 0.01986 g C $m^{-2}a^{-1}$ for each meter. This minimal variation indicates that the ANPP rate is steady, potentially because of specific climatic conditions for example moderate temperatures and consistent precipitation patterns, as well as stable soil types that support sustained vegetation growth (Zhao et al., 2019).

Finally, the ANPP in the highest elevation range (2800-5200 m) showed a significant negative correlation with the increase in elevation. The trend was established to be at the rate of -0.17077 g C $m^{-2}a^{-1}$ with R^2 0.9053 and $p < 0.001$ (Fig. 9B). The decline in ANPP highlights the harsh conditions that hinder growth at the highest elevations such as temperature extremes, reduced atmospheric pressure, and limited soil fertility. The ANPP in the research was realized to have first significantly increased from the lower to mid-elevation zones, stability with slight fluctuations within the higher elevation zones then a significant decrease at the highest elevation zone. Therefore, this pattern manifested the importance of elevation on the distribution of the ANPP temporally and spatially with productivity of highest regression at the mid-elevation and reduced at the highest elevation.

3.4. Correlation between climatic variables and anpp across elevation gradients

The comprehensive pixel-wise correlation analysis evaluating the relationships between ANPP and two key climatic factors, precipitation and temperature, across different vegetation types provides a nuanced insight into ecological responses (Mehmood et al., 2024a; Mehmood et al., 2024d). This analysis includes significant positive ($p<0.05$), significant negative ($p<0.05$), non-significant positive ($p>0.01$), and non-significant negative ($p>0.01$) correlations across six types of vegetation (Fig. 10C). For precipitation, ENT display a clearly relationship, as a vast majority 72.322% or 11,013.87 km^2 presented significant positive correlation between ANPP and precipitation (Fig. 10A). This indicates a critical role of water availability in these forests. Similarly, EBT show an overwhelming positive correlation in 94.967% (812.564 km^2) of their area, emphasizing the essential role precipitation plays in sustaining productivity. Deciduous vegetation types and grasslands also show a predominantly positive relationship but with various levels of strength and significance which in turn indicates that precipitation promotes productivity, but the strength of this relationship can be modified by other ecological or microclimatic factors.

However, the correlation of ANPP with temperature yields more diverse results. ENT and EBT show significant negative correlations over large areas (63.95% or 9,739.2 km^2 for ENT), indicating that lower

temperatures favor productivity, likely due to these species' adaptations to cooler climates (Fig. 10B). DNT and Shrubs also exhibit a significant negative correlation (64.09% or 1,472.42 km^2 for DBT), supporting the notion that cooler temperatures benefit these types. However, DNT and Grasslands display a more complex relationship with temperature. A substantial portion of Grasslands exhibits non-significant positive correlations (36.09% or 8,424.87 km^2), suggesting that these ecosystems might be more resilient or adaptable to warmer conditions, reflecting the ecological diversity and adaptive capacity of these species. The findings are representative of the complex relationship between genetic adaptation, ecological conditions, and the climatic escalation across diverse vegetation types. Some of the vegetation types are strongly predisposed to cool conditions, while others exhibit response variability and a mixture of both temperature and precipitation. In general, the integrated data on the influence of climatic escalation on ecological productivity is significant for the prediction, examination, and regulation of the global climatic changes and their consequences for diverse types of ecosystems.

3.5. Climatic impacts on ANPP across elevation: temperature and precipitation dynamics

The relationship between temperature, precipitation, and ANPP is essential for understanding how elevation influences changes in these climatic variables. Although temperature exhibits a consistent decrease with an increase in elevation as shown by a significant negative correlation ($p < 0.01$) with a decline of about 0.0078°C per meter. The analysis of ANPP shows that, contrary to decreasing temperatures, productivity tends to increase. Specifically, ANPP increases by approximately 3.51 g C/m^2/yr. with each one-degree Celsius increase in temperature (Eq. 21). However, this relationship may not be linear, as extreme temperatures can negatively impact plant physiological processes, potentially reducing productivity. For instance, high temperatures can lead to increased respiration rates, water stress, and heat damage, which can all adversely affect plant growth (Devireddy et al., 2021). Studies have shown that beyond certain thresholds, temperature increases can result in reduced photosynthetic efficiency and higher mortality rates in plants, highlighting the importance of considering these factors to fully understand the dynamic between temperature and ANPP (Raza et al., 2023).

$$\text{ANPP} = 836.88 + 3.51 \times \text{Temperature} + 1.59 \times \text{Precipitation} \quad (21)$$

The regression equation was derived using multiple linear regression analysis. This method quantifies the relationship between ANPP and the independent variables of temperature and precipitation. The coefficients represent the ANPP change for a unit change in the respective climatic variable, holding the other variable constant. Specifically, the coefficient 3.51 indicates that ANPP increases by approximately 3.51 g C/m^2/yr for each one-degree Celsius increase in temperature, while the coefficient 1.59 suggests that ANPP increases by about 1.59 g C/m^2/yr for each additional millimeter of precipitation. These values were obtained through statistical analysis of the collected data, ensuring the model's accuracy in predicting ANPP based on climatic conditions.) Precipitation exhibits a more complex pattern. Initially, precipitation increases with elevation, reaching a peak around mid-elevation zones, before declining towards higher elevations. This pattern is quantified by a weak negative correlation ($r = -0.284$, $p < 0.05$), suggesting a slight decrease but with significant variability. Regression analysis reveals a minor negative trend, with precipitation decreasing by about 0.0157 mm per meter of elevation gain, as shown in Fig. 11. Moreover, the initial increase and subsequent decrease in precipitation align with the regression analysis finding that ANPP is expected to increase by about 1.59 g C/m^2/yr. as precipitation increases.

The findings presented clearly emphasize the complex relationship between elevation, temperature, precipitation, and ecological productivity. The decrease in temperature with elevation, which has been observed in most mountainous areas, is not equally associated with the decline in ecological productivity. ANPP is better linked to changes in temperature and precipitation, regardless of the overall decrease in temperature. This detailed understanding is essential for predicting vegetation dynamics and developing conservation and resource management strategies in mountainous areas.

3.6. Validation of GPP and ANPP using the EC-LUE model

The GPP accuracy calculations obtained from the EC-LUE model were confirmed using a two-step validation analysis. Firstly, the model-calculated GPP results were compared with the product GPP sourced from MODIS Terra dataset (MOD17A3HGF). This step aimed to confirm the precision of the computational techniques and the appropriateness of the model results. The model-derived GPP strongly correlated with the reference GPP data, indicated by an R^2 value of 0.82 ($p < 0.01$) (Fig. 3). This outcome validated the efficiency of the model settings and input parameters. Following a product comparison, NPP estimates were obtained from biomass measurements of selected field plots. These estimates were based on field-derived NPP values collected across 15 diverse sites, which provided a ground-truth assessment of the ecological modeling. Above-ground biomass was harvested (Luo et al., 2024; Anees et al., 2024a) and analyzed for carbon content from six 2 m^2 plots at each site. The carbon measurements were then used to derive ANPP, which was compared with the model's ANPP calculations and the standard product ANPP.

The results obtained from these comparisons further supported the model's validity. When the calculated ANPP was compared with field-derived NPP, the R^2 was 0.78, significantly higher than the 0.75 R^2 obtained from comparing the product ANPP with field-derived NPP (Fig. 4 A & B). As a result, the EC-LUE model has the potential to provide a more precise ANPP simulation than existing product-based estimates. The model's accuracy in estimating GPP and ANPP is demonstrated by this methodical approach to validation, which underscores its potential for enhanced precision in ecological assessments.

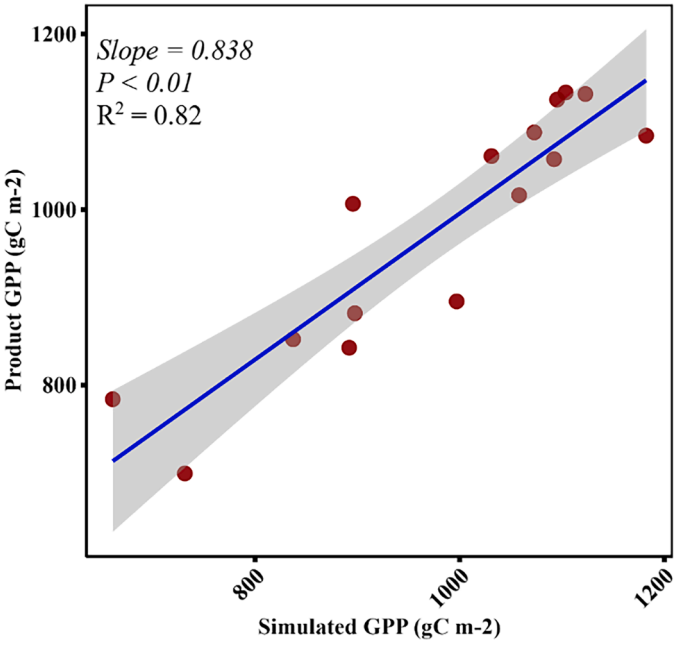

Fig. 3. Comparison of Simulated GPP Outputs from the EC-LUE Model with Product GPP Measurements.

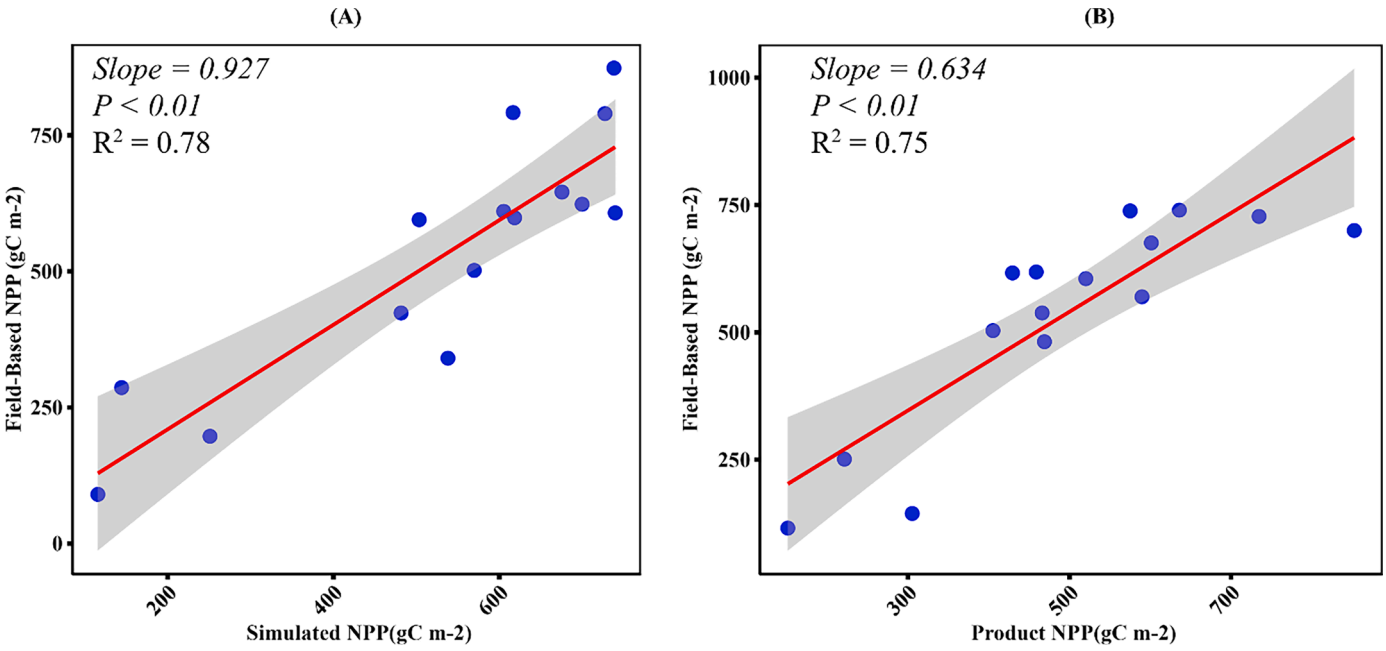

Fig. 4. Comparative Analysis of NPP: (a) NPP Simulated Data, (b) Product NPP Data, and Field-Derived NPP Measurements.

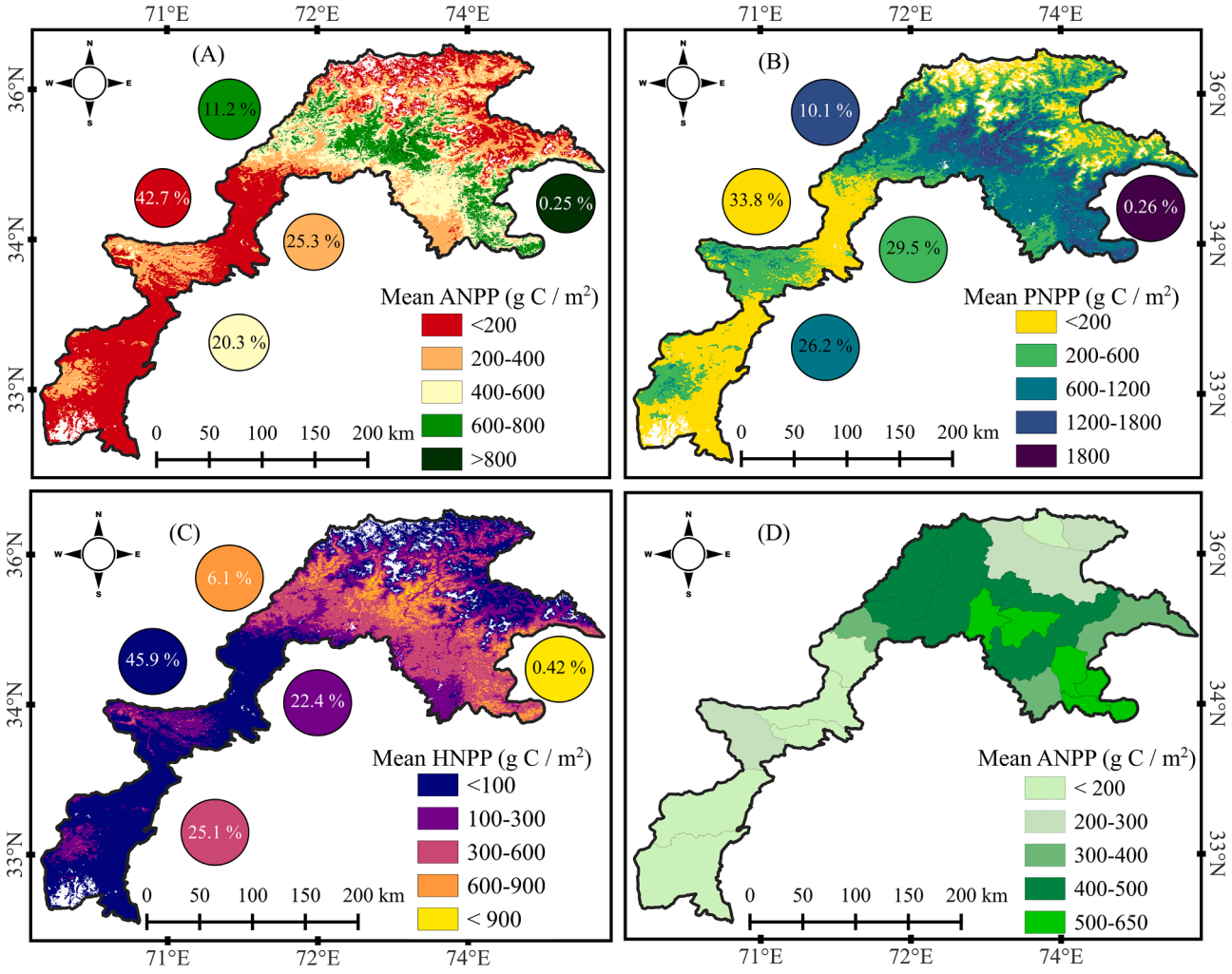

Fig. 5. Spatial Variability of NPP Metrics: The figure illustrates the mean spatial distribution of (A) ANPP, (B) PNPP, (C) HNPP across the study region, and (D) the ANPP recalculated after performing zonal statistics by province.

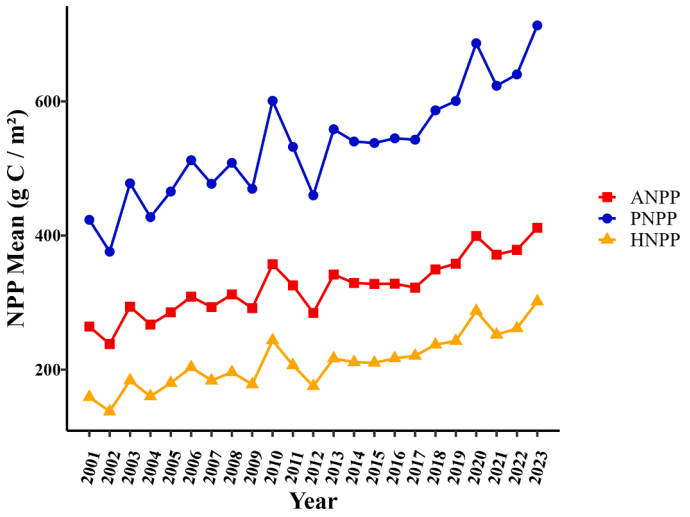

Fig. 6. Interannual Trends of ANPP, PNPP, and HNPP from 2001 to 2023.

4. Discussion

4.1. Environmental and human impacts on NPP (2001-2023)

Our research findings highlight significant differences in the environment and the human actions effect on NPP across different ecological regions between 2001 and 2023. Specifically, the mean ANPP in our study area was 323.46 g C m^{-2} a^{-1}, with an annual increase of 5.73 g C m^{-2} a^{-1}. In contrast, PNPP was significantly higher, averaging 534.99 g C m^{-2} a^{-1}, with a prominent annual increase of 11.058 g C m^{-2} a^{-1}. The difference highlights an increasing range between the potential and actual productivity, which suggests that there is untapped ecological potential that human activities or environmental stressors may cause. The ANPP in croplands across China has increased by an average rate of 3.68 g C m^{-2} a^{-1} between 2000 and 2015. This increase can be attributed to a combination of climate change and human activities. It is important to note that human activities had a relatively minor impact on this increase, contributing only 0.45 g C m^{-2} a^{-1} (Yan et al., 2020). The central Asia ecotone zone exhibited changes in ANPP. The average increases in PNPP, HNPP, and ANPP were 4.71, 3.08, and 1.63 g C m^{-2} a^{-1}, respectively. These changes were a result of climate (Usoltsev et al., 2020; Usoltsev et al., 2022) and human activities that impacted various vegetation and altitude zones differently. Our observations of the productivity of different regions also showed that similar factors influenced productivity differently in different areas (H. Li et al., 2021; Teng et al., 2020; X. Zhou et al., 2022). In addition, our research demonstrated that the regions with extremely high productivity are sparse, making up only 0.25% of the entire area with ANPP exceeding 800 g C m^{-2} a^{-1}. This finding aligns with an overall increasing pattern in vegetation NPP throughout China, highlighting the possibility of rehabilitation in various ecosystems (Feng et al., 2019; Wang et al., 2021). Their research revealed a constant positive shift in NPP, emphasizing the impact of improved meteorological conditions and efficient ecological management.

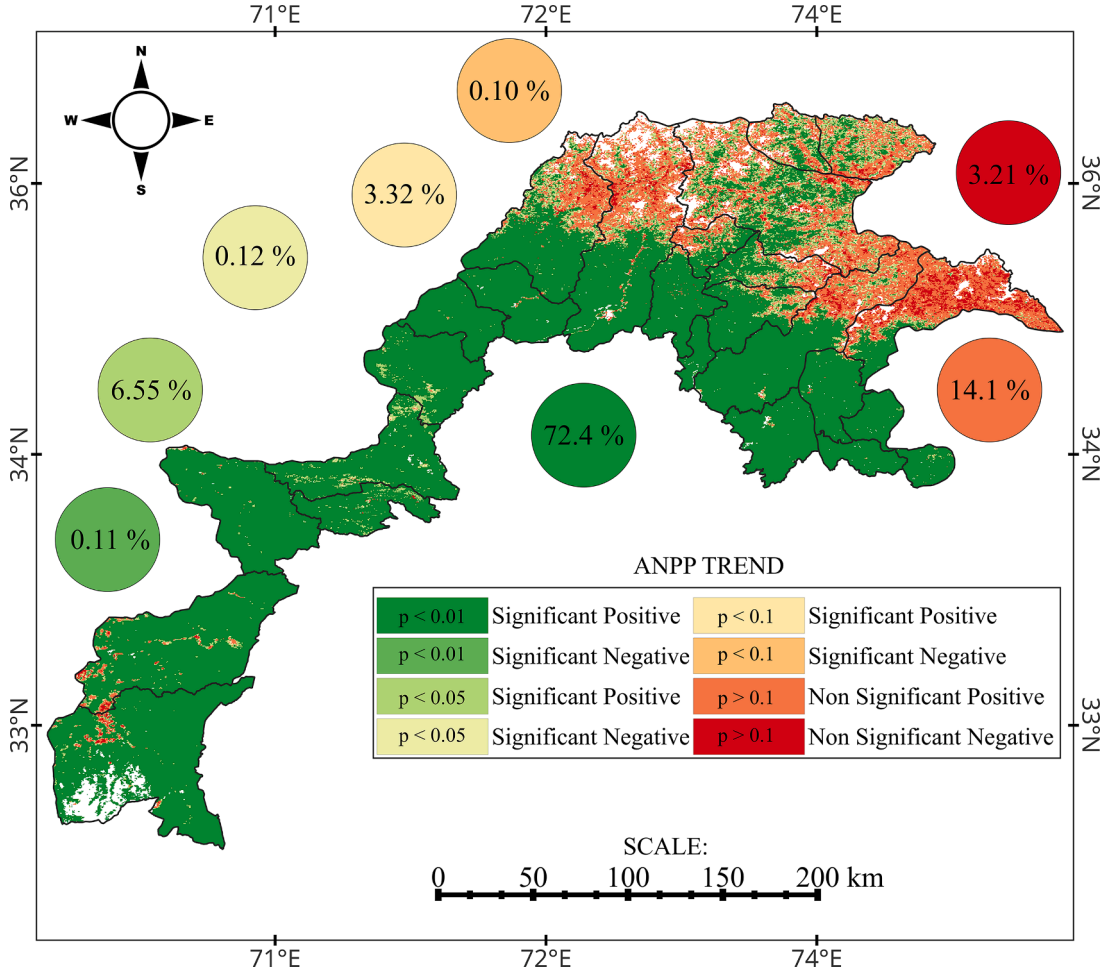

Fig. 7. Mann-Kendall Trend Analysis of ANPP with Various Significance Level, depicted over a spatial gradient for the period 2001 to 2023.

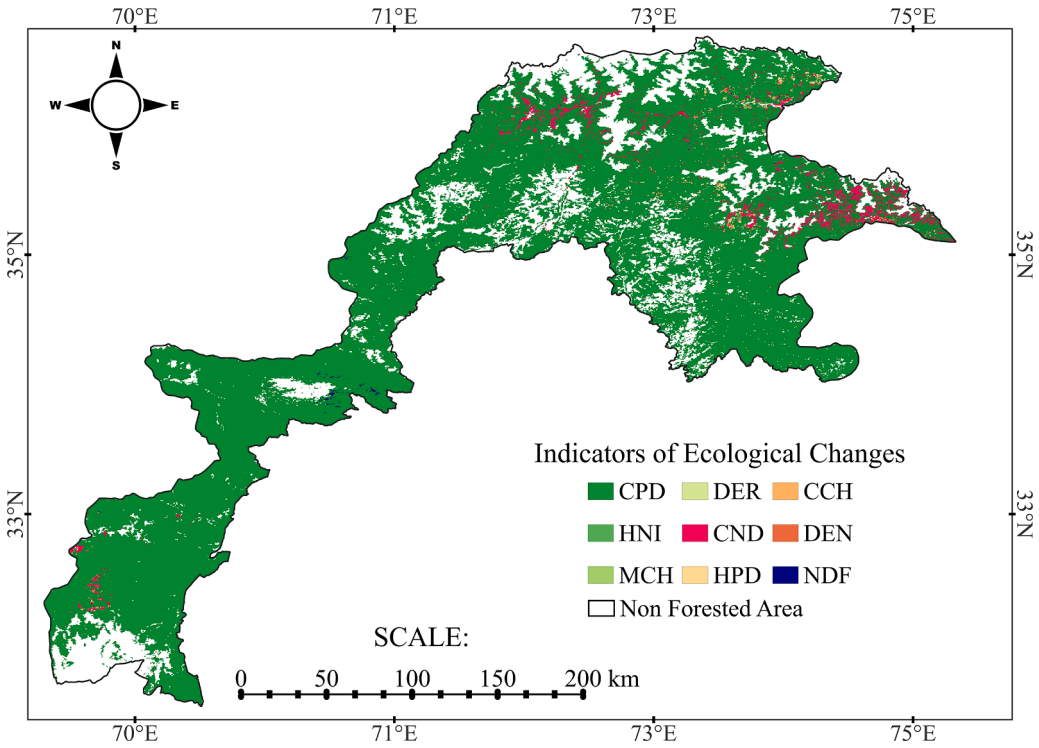

Fig. 8. Distribution of NPP Change Indicators in a Forested Landscape, Classified by Ecological and Anthropogenic Factors.

4.2. Impacts of conservation efforts and technological advances in environmental monitoring

A positive trend in ANPP across 72.44% of the region was significantly impacted by the Billion Trees Afforestation Project (BTAP) initiated in 2014, highlighting the impacts of conservation efforts (Shafeeque et al., 2022; Ullah et al., 2020) . In contrast, a small fraction (0.11%) of the area showed a substantial negative trend in ANPP, likely due to deforestation and urban expansion Teng et al. (2020). Areas with less pronounced positive trends ($p < 0.05$ and $p < 0.10$) indicate subtle improvements or stages of early recovery on the potential for targeted management. Finally, zones with non-significant trends, which constitute 17.34% of the study area, suggest stability in ANPP, which is crucial for sustaining ecosystem services (Chen et al., 2022; Xu et al., 2019). The majority (95.1%) of the area has been affected by climate factors (Shobairi et al., 2022), leading to significant changes in productivity that fall under CPD scenarios. This classification encompasses positive changes in productivity, emphasizing its considerable impact on regions that contribute to ecological health. These regions have critical part in conserving biodiversity and supporting carbon sequestration, underscoring their crucial importance in ecological conservation. Only a slight fraction, 0.15%, exhibited human impact (HNI), indicating sites where human actions like urban growth, deforestation, and unsustainable farming methods are causing a decrease in productivity. This finding is vital in identifying areas that require intervention to reduce the negative effects.

Recent studies have demonstrated the efficacy of advanced remote sensing and machine learning techniques in monitoring environmental changes and urban dynamics (Luo et al., 2024; Anees et al., 2024a; Mehmood et al., 2024a; Shahzad et al., 2024). For instance, the assessment of spatiotemporal characteristics of droughts using remote sensing-based indices, such as soil moisture condition index (SMCI) and vegetation condition index (VCI), has proven critical in evaluating drought conditions over extended periods (Jalayer et al., 2023). Similarly, the application of convolutional neural networks (CNNs) in urban mapping using very high resolution (VHR) satellite images has highlighted the importance of texture information in land cover/land use (LULC) classification (Hussain et al., 2024b), particularly when compared to traditional machine learning methods (Anees et al., 2024a; Luo et al., 2024; Mohammadi & Sharifi, 2021; Mehmood et al., 2024a; Badshah et al., 2024). Moreover, the monitoring of nitrogen dioxide (NO2) pollution levels during the coronavirus pandemic using Sentinel-5P satellite imagery has provided valuable insights into the impact of reduced industrial activities and traffic on air quality (Sharifi & Felegari, 2022). These studies underscore the growing importance of integrating remote sensing data with machine learning algorithms to effectively monitor and manage environmental conditions across different scales and settings (Anees et al., 2024a; Luo et al., 2024; Mehmood et al., 2024a).

4.3. Influence of elevation, temperature, and precipitation on NPP dynamics

The distribution of NPP in an area is significantly influenced by elevation. Our study found that in the (0-400 meters) zone, there is a mild positive correlation between ANPP and elevation. At lower elevations, higher ANPP is favored due to the more favorable temperature and nutrient availability (Long et al., 2023; Piton et al., 2020). A strong positive trend in ANPP has been observed at mid-elevations (401-1600 meters), which aligns with findings of similar patterns in a Mediterranean beech forest (Miranda et al., 2022; Zianis and Mencuccini, 2005). The optimal conditions for ANPP appear to be at mid-elevations before reaching higher elevations, where productivity is limited by factors such as decreased temperature and increased wind exposure. ANPP showed minimal changes at higher elevations (1600-2800 meters), indicating a threshold beyond which environmental stressors begin to dominate. High-elevation meadows have reduced soil moisture and a shorter growing season, which suggest similar limitations across different high-elevation ecosystems (Snyder et al., 2023). Above 2800 meters, we found a significant negative correlation between elevation and ANPP, indicating the harsh climatic conditions that hinder vegetation growth. Reduced growth efficiency and ANPP at high elevations are due to

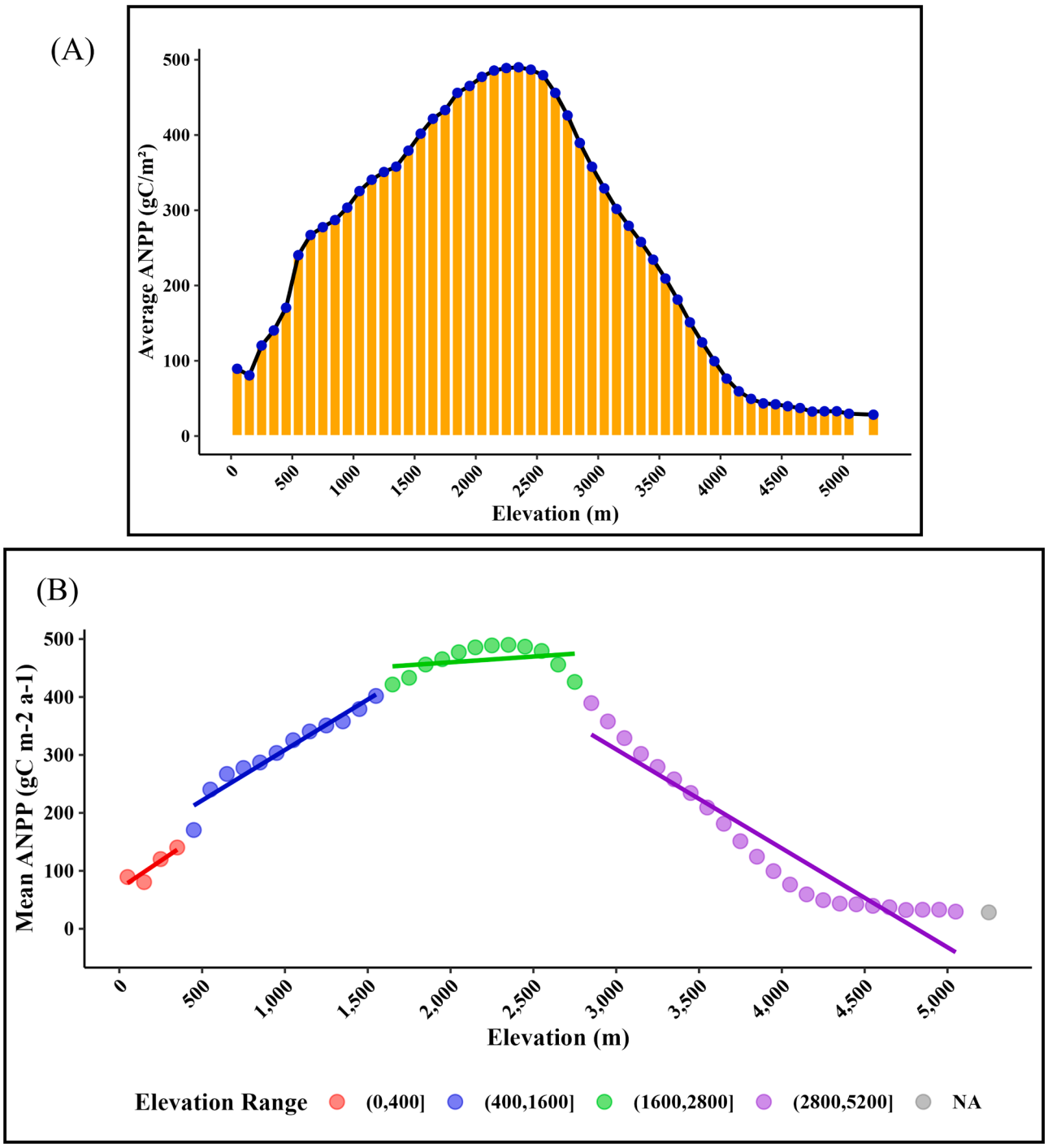

Fig. 9. (A) Distribution of Average ANPP across Elevation Bands (100m Intervals). The graph displays the mean ANPP (in g C/m^2/yr) plotted against the 100-meter elevation band, ranging from 0 to 5000 meters. (B) Predictive Analysis of Mean ANPP by Elevation Range Using Linear Models.

factors such as strong winds and colder temperatures (Y. Zhang et al., 2021). The findings indicate that the NPP is greatly influenced by altitude. At first, ANPP experiences a significant rise in the lower to mid-elevation areas. It remains relatively constant with minor changes at higher elevations and eventually decreases sharply in the highest elevation zones (Song et al., 2022; Zhao et al., 2021).

Our research reveals that there is a strong positive connection between precipitation and ANPP in ENT and EBT that covers 72.322% and 94.967% of their respective regions. Thus, moisture availability, which is critical for photosynthesis, is improved by precipitation, significantly influencing the productivity of forest ecosystems (Lian et al., 2023; X. Zhang et al., 2024). Grasslands and deciduous ecosystems display a positive but varying relationship, with grassland ANPP responding positively to increased precipitation across different climatic zones (Curcio et al., 2023; Shi et al., 2023). This research shows that ENT and EBT have significant negative correlations with temperature, suggesting that cooler temperatures are favorable for productivity, most likely due to genetic adaptations. Higher temperatures often lead to decreased productivity in forest ecosystems due to respiratory losses surpassing gains from photosynthesis (Perez-Quezada et al., 2023). On the other hand, grasslands exhibited non-significant positive correlations with temperature, demonstrating resilience to warmer conditions. Grasslands

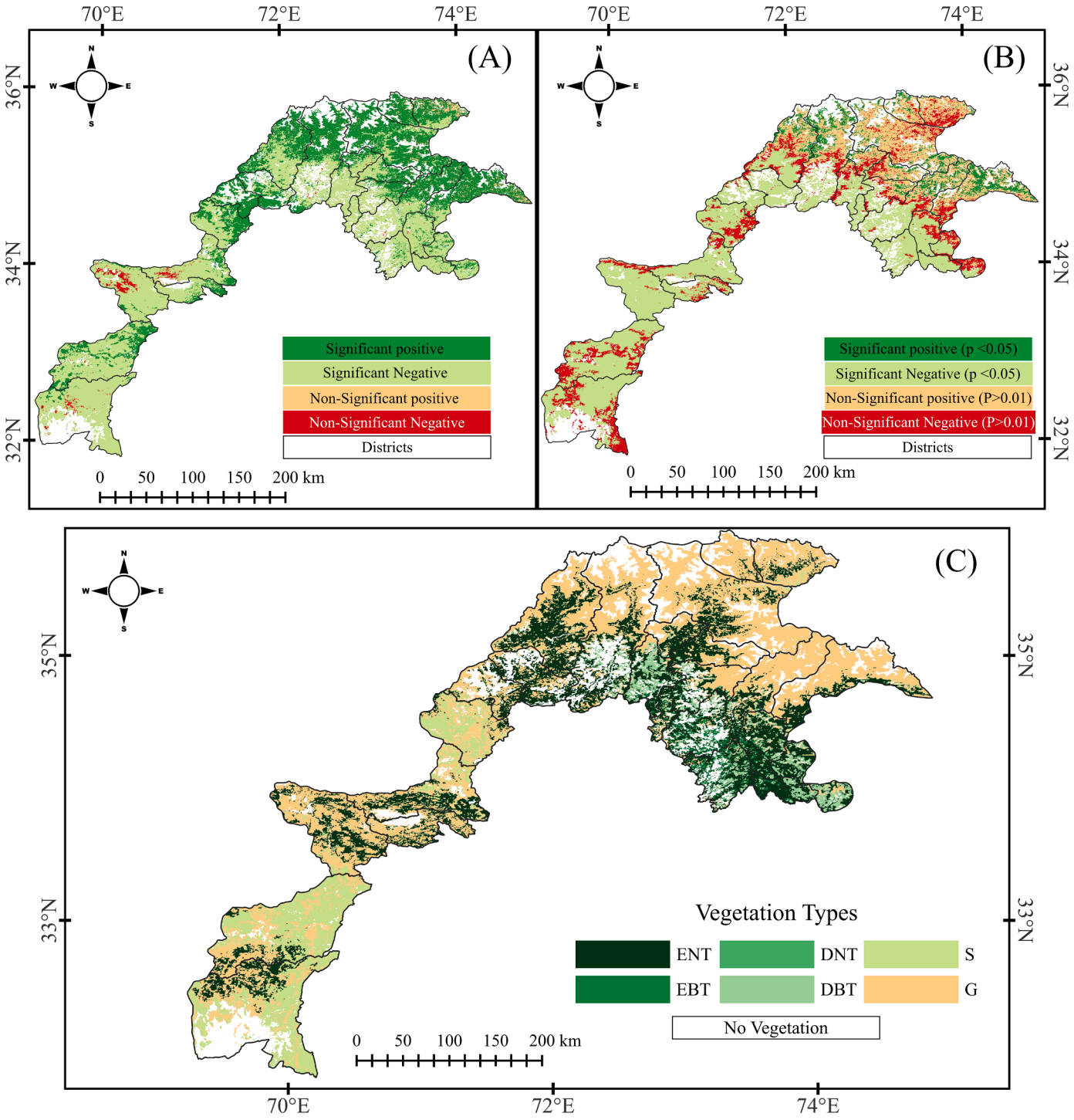

Fig. 10. Spatial correlation analysis between ANPP and climatic factors across various vegetation types: (A) the correlation between ANPP and precipitation, highlighting areas of significant and non-significant relationships. (B) ANPP and temperature, (C) represents the distribution of different vegetation types in the region.

adapted to increased temperatures, likely due to phenotypic plasticity and genotypic diversity within these ecosystems. The variability in ANPP is influenced by the complex pattern of precipitation, which is affected by local geography and atmospheric conditions at different elevations. While there is only a slight overall decrease in precipitation with elevation, the peaks at mid-elevations, which correspond to higher ANPP values, indicate regions with potentially optimal ecological productivity.

There is a negative correlation between elevation and temperature, where temperature decreases by 0.0078°C per meter with an increase in elevation. It is in line with climatological principles, as temperature typically decreases with altitude due to the expansion of air in the atmosphere, leading to cooling effects (Vacek et al., 2023). However, observing an increase in ANPP with temperature contradicts typical expectations. Typically, cooler temperatures at higher elevations might limit photosynthetic activity and plant growth. This unexpected relationship suggests that other factors might be at play, such as microclimatic conditions or adaptation strategies of mountainous flora, which

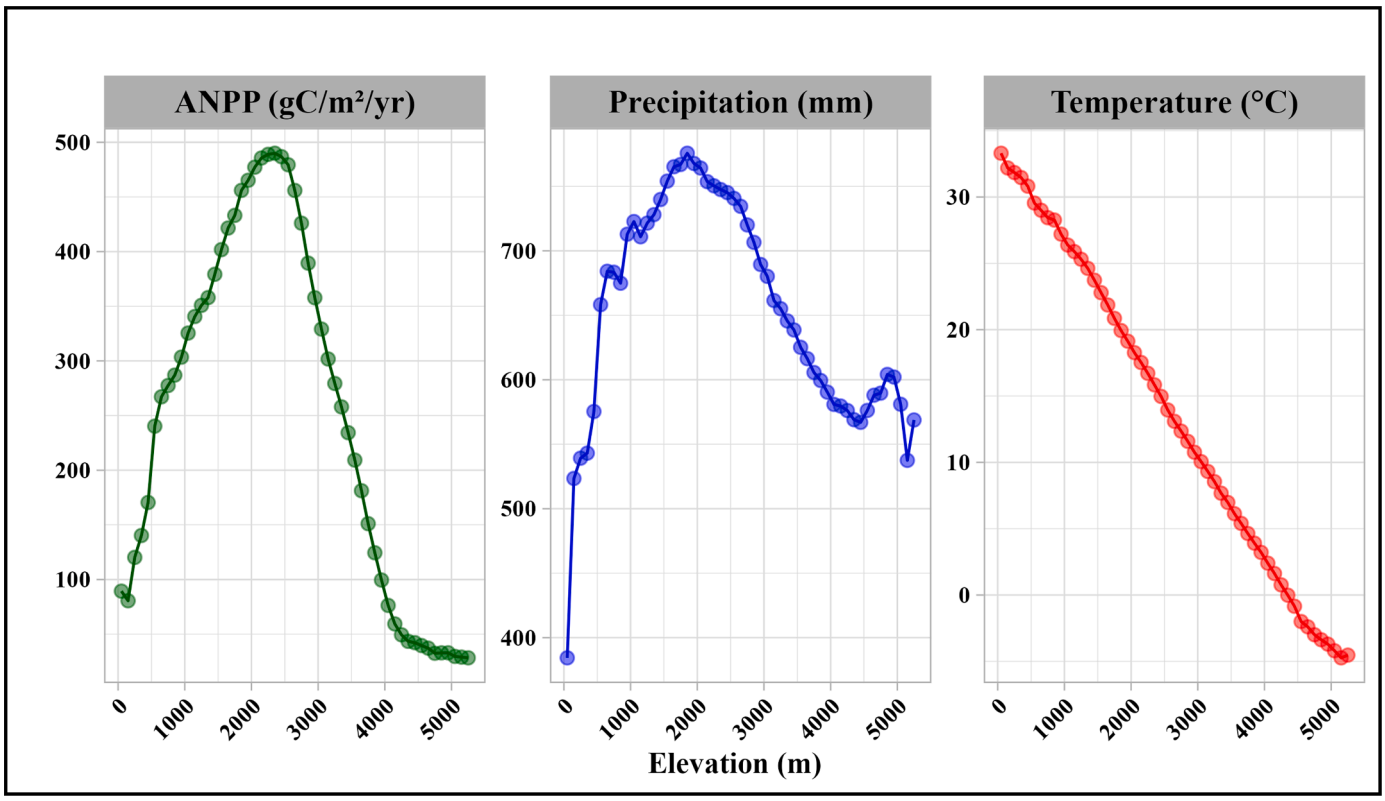

Fig. 11. Relationship between elevation and climatic variables alongside ANPP.

could mitigate the direct impacts of lower temperatures. For instance, Photosynthesis is usually enhanced due to increased solar radiation, reduced cloud cover, or lesser atmospheric interference at higher altitudes, which could boost productivity despite lower temperatures (Z. Liu et al., 2023). The relationship between ANPP and precipitation exhibits a non-linear pattern. Typically, precipitation increases with elevation until it reaches a peak and then starts to decrease. The trend is supported by a statistically significant, negative correlation with a decrease rate of 0.0157 mm per meter of elevation gain. The orographic effect can be attributed to this pattern, where mountains act as obstacles to air movement, causing precipitation to rise on the windward side and decline after crossing over the ridge (He et al., 2024; M. Zhang et al., 2024). The observed increase in ANPP with precipitation highlights the critical role of water availability in sustaining productivity, especially in mountainous environments where moisture may limit biological activity. A thorough understanding of local climate dynamics can be obtained by regressing ANPP with temperature and precipitation in combination with elevation gradient analysis. It shows how ecological productivity is dictated by microclimatic conditions, which are influenced by both temperature and precipitation. The research covers a substantial time interval from 2001 to 2023. However, it is crucial to consider that the annual resolution applied could hide even more detailed seasonal tendencies, which could be essential for understanding the NPP dynamics. Even though our study supported by (Huang et al., 2023; X. Zhou et al., 2022) in emphasizing the significance of the human factor (Hussain et al., 2024a) for NPP, it is hard to measure the effect of deforestation accurately. It relies on the natural system's inherent variability.

4.4. Limitations of the study

While our study provides valuable insights, it is important to acknowledge certain limitations. The spatial and temporal resolution of the remote sensing datasets (e.g., MODIS, ERA5) may affect the precision of our estimates, particularly in areas with complex terrain or rapidly changing conditions. Additionally, although key climatic variables such as temperature and precipitation were included, other factors like soil properties, land management practices, and biotic interactions, which could influence NPP, were not explicitly modeled. The availability and quality of remote sensing data, along with gaps in in-situ measurements, further limit the accuracy and validation of our estimates. These factors should be considered when interpreting our findings and highlight areas for future research to enhance the robustness of the results.

4.5. Outlook for Future Research

Future research should aim to address the limitations identified in this study by incorporating higher-resolution datasets and expanding the range of environmental variables considered. Additionally, exploring seasonal and finer temporal dynamics of NPP could provide a more detailed understanding of productivity changes. Investigating the impact of land management practices and biotic interactions on NPP will also enhance the robustness of future studies.

5. Conclusion

This research provides a detailed analysis of Net Primary Productivity (NPP) in northern Pakistan across different elevations, highlighting the significant influence of elevation and climatic conditions on vegetation productivity. Over the study period from 2001 to 2023, we observed an average annual NPP of 323.46 g C m^{-2} a^{-1}, with an annual increase of 5.73 g C m^{-2} a^{-1}. These findings underscore the adaptability of the region's vegetation to climatic changes and emphasize the critical importance of mid-elevation areas for high productivity. Our study demonstrates the effectiveness of advanced remote sensing and ecological models, particularly the EC-LUE model, which shows a strong correlation ($R2 = 0.82$) with MODIS-derived GPP. This approach significantly enhances our understanding of ecological processes, offering high precision in capturing environmental dynamics and providing a robust foundation for future

research and model validation. However, it is important to acknowledge the limitations of our work, such as the spatial and temporal resolution constraints of the remote sensing datasets and the exclusion of other environmental factors like soil properties and land management practices. These limitations suggest areas for further research, including the need for more comprehensive modeling that incorporates these additional factors. Looking ahead, future research should focus on refining these models to improve the accuracy of NPP predictions, particularly in regions with complex terrains and rapidly changing environmental conditions. Additionally, there is a need for more in-depth scenario-based evaluations that consider the varying impacts of climatic factors on different vegetation types and elevation zones. Such research will be crucial in informing integrated ecological management and conservation strategies that are responsive to the challenges posed by global environmental changes. This study contributes valuable insights into NPP dynamics and underscores the urgent need for targeted conservation efforts, especially in mid-elevation areas where productivity peaks. The findings also highlight the importance of informed policymaking to sustain the health and productivity of forest ecosystems in the face of ongoing climatic shifts. Eq. (1)-(2), Eq. (7)-(10), Eq. (16)-(17), Eq. (19)-(20)

Ethics approval and consent to participate

Not Applicable.

Consent for publication

Not Applicable.

CRediT authorship contribution statement

Kaleem Mehmood: Writing – review & editing, Writing – original draft, Visualization, Validation, Software, Methodology, Investigation, Formal analysis, Data curation, Conceptualization. **Shoaib Ahmad Anees:** Writing – review & editing, Writing – original draft, Visualization, Validation, Supervision, Software, Methodology, Investigation, Formal analysis, Data curation, Conceptualization. **Akhtar Rehman:** Writing – review & editing. **Nazir Ur Rehman:** Writing – review & editing. **Sultan Muhammad:** Writing – review & editing. **Fahad Shahzad:** Writing – review & editing. **Qijing Liu:** Writing – review & editing. **Sulaiman Ali Alharbi:** Writing – review & editing. **Saleh Alfarraj:** Writing – review & editing. **Mohammad Javed Ansari:** Writing – review & editing. **Waseem Razzaq Khan:** Writing – review & editing, Investigation, Formal analysis.

Declaration of competing interest

The authors declare that they have no known competing financial interests or personal relationships that could have appeared to influence the work reported in this paper.

Data availability

The authors confirm that the data links supporting the findings of this study are available within the article.

Acknowledgements

We are grateful to the Key Laboratory for Silviculture and Conservation of Ministry of Education, Beijing Forestry University, Beijing, (100083), P. R. China, for providing assistance and platforms for this research. We are also grateful to the Department of Forestry, The University of Agriculture, Dera Ismail Khan, 29050, Pakistan, for providing assistance and platforms for this research. This project was supported by Researchers Supporting Project Number (RSP2025R7) King Saud University, Riyadh, Saudi Arabia. Authors also acknowledge the support of the Universiti Putra Malaysia.

Supplementary materials

Supplementary material associated with this article can be found, in the online version, at doi:10.1016/j.tfp.2024.100657.

References

Ahmed, S., 2011. Does economic geography matter for Pakistan? A spatial exploratory analysis of income and education inequalities. Pak. Dev. Rev. 50 https://doi.org/10.30541/v50i4iipp.929-953.

Akram, M., Hayat, U., Shi, J., Anees, S.A., 2022. Association of the female flight ability of asian spongy moths (lymantria dispar asiatica) with locality, age and mating: a case study from China. Forests. 13 (8), 1158. https://doi.org/10.3390/f13081158.

Ali, R., Rashid Abubaker, S., Othman Ali, R., 2019. Trend analysis using mann-kendall, sen's slope estimator test and innovative trend analysis method in Yangtze river basin, china: review. Int. J. Eng. Technol. 8.

Allen, K., Bellingham, P.J., Richardson, S.J., Allen, R.B., Burrows, L.E., Carswell, F.E., Husheer, S.W., St. John, M.G., Peltzer, D.A., 2023. Long-term exclusion of invasive ungulates alters tree recruitment and functional traits but not total forest carbon. Ecol. Appl. 33 https://doi.org/10.1002/eap.2836.

An, H., Zhai, J., Song, X., Wang, G., Zhong, Y., Zhang, K., Sun, W., 2024. Impacts of extreme precipitation and diurnal temperature events on grassland productivity at different elevations on the Plateau. Remote Sens. (Basel) 16. https://doi.org/10.3390/rs16020317.

Andreevich, U.V., Reza, S.S.O., Stepanovich, T.I., Amirhossein, A., Meng, Z., Anees, S.A., Petrovich, C.V., 2020. Are there differences in the response of natural stand and plantation biomass to changes in temperature and precipitation? A case for two-needled pines in Eurasia. J. Resour. Ecol. 11 (4), 331. https://doi.org/10.5814/j.issn.1674-764x.2020.04.001.

Anees, S.A., Mehmood, K., Khan, W.R., Sajjad, M., Alahmadi, T.A., Alharbi, S.A., Luo, M., 2024a. Integration of machine learning and remote sensing for above ground biomass estimation through Landsat-9 and field data in temperate forests of the Himalayan region. Ecol. Inform., 102732 https://doi.org/10.1016/j.ecoinf.2024.102732.

Anees, S.A., Yang, X., Mehmood, K., 2024b. The stoichiometric characteristics and the relationship with hydraulic and morphological traits of the Faxon fir in the subalpine coniferous forest of Southwest China. Ecol. Indic. 159, 111636 https://doi.org/10.1016/j.ecolind.2024.111636.

Anees, S.A., Zhang, X., Khan, K.A., Abbas, M., Ghramh, H.A., Ahmad, Z., 2022a. Estimation of fractional vegetation cover dynamics and its drivers based on multi-sensor data in Dera Ismail Khan. Pakistan. J King Saud Univ Sci 34. https://doi.org/10.1016/j.jksus.2022.102217.

Anees, S.A., Zhang, X., Shakeel, M., Al-Kahtani, M.A., Khan, K.A., Akram, M., Ghramh, H. A., 2022b. Estimation of fractional vegetation cover dynamics based on satellite remote sensing in pakistan: A comprehensive study on the FVC and its drivers. J. King. Saud. Univ. Sci. 34 https://doi.org/10.1016/j.jksus.2022.101848.

Aslam, M.S., Huanxue, P., Sohail, S., Majeed, M.T., Rahman, S.U., Anees, S.A., 2022. Assessment of major food crops production-based environmental efficiency in China, India, and Pakistan. Environ. Sci. Pollut. Res. 1–10. https://doi.org/10.1007/s11356-021-16161-x.

Badshah, M.T., Hussain, K., Rehman, A.U., Mehmood, K., Muhammad, B., Wiarta, R., Meng, J., 2024. The role of random forest and Markov chain models in understanding metropolitan urban growth trajectory. Front. For. Glob. Change 7, 1345047.

Bakiev, M., Khasanov, K., Primbetov, I., 2022. Vertical accuracy of freely available global digital elevation models: a case study in karaman water reservoir territory. Int. J. Geoinf. 18 https://doi.org/10.52939/ijg.v18i1.2107.

Bi, M., Wan, L., Zhang, Z., Zhang, X., Yu, C., 2023. Spatio-temporal variation characteristics of North Africa's. Climate Potential Product.. Land (Basel) 12. https://doi.org/10.3390/land12091710.

Black, K., Lanigan, G., Ward, M., Kavanagh, I., hUallacháin, D., Sullivan, L.O., 2023. Biomass carbon stocks and stock changes in managed hedgerows. Sci. Total Environ. 871 https://doi.org/10.1016/j.scitotenv.2023.162073.

Chen, S., Chen, J., Jiang, Chunqian, Yao, R.T., Xue, J., Bai, Y., Wang, H., Jiang, Chunwu, Wang, S., Zhong, Y., 2022. Trends in research on forest ecosystem services in the most recent 20 years: A bibliometric analysis. Forests. 13, 1087.

Chen, S., Ma, M., Wu, S., Tang, Q., Wen, Z., 2023. Topography intensifies variations in the effect of human activities on forest NPP across altitude and slope gradients. Environ. Dev. 45 https://doi.org/10.1016/j.envdev.2023.100826.

Chen, X., Wang, Y., Chen, Y., Fu, S., Zhou, N., 2023. NDVI-Based Assessment of Land Degradation Trends in Balochistan, Pakistan, and Analysis of the Drivers. Remote Sens. (Basel) 15. https://doi.org/10.3390/rs15092388.

Chen, X., Zhang, Y., 2023. Impacts of climate, phenology, elevation and their interactions on the net primary productivity of vegetation in Yunnan, China under global warming. Ecol. Indic. 154 https://doi.org/10.1016/j.ecolind.2023.110533.

Cheng, N., Zhou, Y., He, W., Ju, W., Zhu, T., Liu, Y., Song, P., Bi, W., Zhang, X., Wei, X., 2023. Exploring light use efficiency models capacities in characterizing environmental impacts on paddy rice productivity. Int. J. Appl. Earth Obser. Geoinfor. 117 https://doi.org/10.1016/j.jag.2023.103179.

Cui, L., Shi, J., Xiao, F., 2023. Change and relationship between growing season metrics and net primary productivity in forestland and grassland in China. Carbon Balance Manag 18. https://doi.org/10.1186/s13021-023-00245-x.
Curcio, M., Irisarri, G., García Martínez, G., Oesterheld, M., 2023. Trends of aboveground net primary productivity of patagonian meadows, the omitted ecosystem in desertification studies. Remote Sens. (Basel) 15. https://doi.org/10.3390/rs15102531.
da Costa, A.C.L., Metcalfe, D.B., Doughty, C.E., de Oliveira, A.A.R., Neto, G.F.C., da Costa, M.C., Silva Junior, J.de A, Aragão, L.E.O.C., Almeida, S., Galbraith, D.R., Rowland, L.M., Meir, P., Malhi, Y., 2014. Ecosystem respiration and net primary productivity after 8-10 years of experimental through-fall reduction in an eastern Amazon forest. Plant Ecol. Divers. 7 https://doi.org/10.1080/17550874.2013.798366.
de Sousa, K., Sparks, A., Ashmall, W., van Etten, J., Solberg, S., 2020. chirps: API Client for the CHIRPS Precipitation Data in R. J. Open. Source Softw. 5 https://doi.org/10.21105/joss.02419.
Devireddy, A.R., Tschaplinski, T.J., Tuskan, G.A., Muchero, W., Chen, J.G., 2021. Role of reactive oxygen species and hormones in plant responses to temperature changes. Int. J. Mol. Sci. https://doi.org/10.3390/ijms22168843.
Ding, H., Yuan, Z., Shi, X., Yin, J., Chen, F., Shi, M., Zhang, F., 2023. Soil moisture content-based analysis of terrestrial ecosystems in China: Water use efficiency of vegetation systems. Ecol. Indic. 150 https://doi.org/10.1016/j.ecolind.2023.110271.
Du, D., Jiao, L., Wu, X., Xue, R., Wei, M., Zhang, P., Li, Q., Wang, X., 2024. Drought determines the growth stability of different dominant conifer species in Central Asia. Glob. Planet. Change 234. https://doi.org/10.1016/j.gloplacha.2024.104370.
Esmaeili, M., Abbasi-Moghadam, D., Sharifi, A., Tariq, A., Li, Q., 2023. Hyperspectral image band selection based on CNN embedded GA (CNNeGA). IEEe J. Sel. Top. Appl. Earth. Obs. Remote Sens. 16, 1927–1950.
Fan, X., Liu, Y., Wu, G., Zhao, X., 2020. Compositing the minimum NDVI for daily water surface mapping. Remote Sens. (Basel) 12. https://doi.org/10.3390/rs12040700.
Feng, Y., Zhu, Jianxiao, Zhao, X., Tang, Z., Zhu, Jiangling, Fang, J., 2019. Changes in the trends of vegetation net primary productivity in China between 1982 and 2015. Environ. Res. Lett. 14 https://doi.org/10.1088/1748-9326/ab4cd8.
Frimpong, B.F., Koranteng, A., Molkenthin, F., 2022. Analysis of temperature variability utilising Mann–Kendall and Sen's slope estimator tests in the Accra and Kumasi Metropolises in Ghana. Environ. Syst. Res. (Heidelb) 11. https://doi.org/10.1186/s40068-022-00269-1.
Gallardo, V.B., Hadad, M.A., Roig, F.A., Gatica, G., Chen, F., 2024. Spatio-temporal linkage variations between NDVI and tree rings on the leeward side of the northern Patagonian Andes. For. Ecol. Manage 553. https://doi.org/10.1016/j.foreco.2023.121593.
Gan, R., Zhang, Y., Shi, H., Yang, Y., Eamus, D., Cheng, L., Chiew, F.H.S., Yu, Q., 2018. Use of satellite leaf area index estimating evapotranspiration and gross assimilation for Australian ecosystems. Ecohydrology. 11 https://doi.org/10.1002/eco.1974.
Gao, W., Wang, H., SPIE (Society), 2008. Remote Sensing and Modeling of Ecosystems for Sustainability V 13 August 2008. San Diego, California, USA. Proceedings of SPIE.
Garba, H., Udokpoh, U.U., 2023. Analysis of Trend in Meteorological and Hydrological Time-series using Mann-Kendall and Sen's Slope Estimator Statistical Test in Akwa Ibom State. Nigeria. Int. J. Environ. Climate Change 13. https://doi.org/10.9734/ijecc/2023/v13i102748.
Gomis-Cebolla, J., Rattayova, V., Salazar-Galán, S., Francés, F., 2023. Evaluation of ERA5 and ERA5-Land reanalysis precipitation datasets over Spain (1951–2020). Atmos. Res. 284 https://doi.org/10.1016/j.atmosres.2023.106606.
Haider, K., Khokhar, M.F., Chishtie, F., RazzaqKhan, W., Hakeem, K.R., 2017. Identification and future description of warming signatures over Pakistan with special emphasis on evolution of CO 2 levels and temperature during the first decade of the twenty-first century. Environ. Sci. Pollut. Res. 24, 7617–7629.
He, C., Braun, J., Tang, H., Yuan, X., Acevedo-Trejos, E., Ott, R.F., Stucky de Quay, G., 2024. Drainage divide migration and implications for climate and biodiversity. Nat. Rev. Earth. Environ. https://doi.org/10.1038/s43017-023-00511-z.
He, L., Rosa, L., Lobell, D.B., Wang, Y., Yin, Y., Doughty, R., Yao, Y., Berry, J.A., Frankenberg, C., 2023. The weekly cycle of photosynthesis in Europe reveals the negative impact of particulate pollution on ecosystem productivity. Proc. Natl. Acad. Sci. u S. a 120. https://doi.org/10.1073/pnas.2306507120.
He, Y., Yan, W., Cai, Y., Deng, F., Qu, X., Cui, X., 2022. How does the Net primary productivity respond to the extreme climate under elevation constraints in mountainous areas of Yunnan, China? Ecol. Indic. 138 https://doi.org/10.1016/j.ecolind.2022.108817.
Hilker, T., Coops, N.C., Wulder, M.A., Black, T.A., Guy, R.D., 2008. The use of remote sensing in light use efficiency based models of gross primary production: A review of current status and future requirements. Sci. Total Environ. 404 https://doi.org/10.1016/j.scitotenv.2007.11.007.
Huang, Q., Zhang, F., Zhang, Q., Jin, Y., Lu, X., Li, X., Liu, J., 2023. Assessing the effects of human activities on terrestrial net primary productivity of grasslands in typical ecologically fragile areas. Biology. (Basel) 12. https://doi.org/10.3390/biology12010038.
Huang, R., Chen, X., Hu, Q., Jiang, S., Dong, J., 2024. Impacts of altitudinal ecohydrological dynamic changes on water balance under warming climate in a watershed of the Qilian Mountains. China. Sci. Total Environ. 908 https://doi.org/10.1016/j.scitotenv.2023.168070.
Huang, X., Xiao, J., Wang, X., Ma, M., 2021. Improving the global MODIS GPP model by optimizing parameters with FLUXNET data. Agric. For. Meteorol. 300 https://doi.org/10.1016/j.agrformet.2020.108314.
Hussain, K., Mehmood, K., Anees, S.A., Ding, Z., Muhammad, S., Badshah, T., Shahzad, F., Haidar, I., Wahab, A., Ali, J., Ansari, M.J., 2024a. Assessing Forest fragmentation due to land use changes from 1992 to 2023: a spatio-temporal analysis using remote sensing data. Heliyon. https://doi.org/10.1016/j.heliyon.2024.e34710.
Hussain, K., Mehmood, K., Yujun, S., Badshah, T., Anees, S.A., Shahzad, F., Nooruddin, Ali, J., Bilal, M., 2024b. Analysing LULC transformations using remote sensing data: insights from a multilayer perceptron neural network approach. Ann. GIS. 1–27. https://doi.org/10.1080/19475683.2024.2343399.
Idoate-Lacasia, J., Stillhard, J., Portier, J., Brang, P., Zimmermann, S., Bigler, C., Bugmann, H., Hobi, M.L., 2024. Long-term biomass dynamics of temperate forests in Europe after cessation of management. For. Ecol. Manage 554. https://doi.org/10.1016/j.foreco.2024.121697.
Ingle, R., Bhatnagar, S., Ghosh, B., Gill, L., Regan, S., Connolly, J., Saunders, M., 2023. Development of hybrid models to estimate gross primary productivity at a near-natural peatland using sentinel 2 data and a light use efficiency model. Remote Sens. (Basel) 15. https://doi.org/10.3390/rs15061673.
Jalayer, S., Sharifi, A., Abbasi-Moghadam, D., Tariq, A., Qin, S., 2023. Assessment of spatiotemporal characteristic of droughts using in situ and remote sensing-based drought indices. IEEe J. Sel. Top. Appl. Earth. Obs. Remote Sens. 16, 1483–1502.
Jallat, H., Khokhar, M.F., Kudus, K.A., Nazre, M., Saqib, N.U., Tahir, U., Khan, W.R., 2021. Monitoring carbon stock and land-use change in 5000-year-old juniper forest stand of Ziarat, Balochistan, through a synergistic approach. Forests. 12 (1), 51.
JAXA, 2019. ALOS Global Digital Surface Model "ALOS World 3D - 30m" (AW3D30). JAXA Data Report.
Junttila, S., Ardö, J., Cai, Z., Jin, H., Kljun, N., Klemedtsson, L., Krasnova, A., Lange, H., Lindroth, A., Mölder, M., Noe, S.M., Tagesson, T., Vestin, P., Weslien, P., Eklundh, L., 2023. Estimating local-scale forest GPP in Northern Europe using Sentinel-2: Model comparisons with LUE, APAR, the plant phenology index, and a light response function. Scie. Remote Sens. 7 https://doi.org/10.1016/j.srs.2022.100075.
Karmakar, P., Teng, S.W., Murshed, M., Pang, S., Li, Y., Lin, H., 2024. Crop monitoring by multimodal remote sensing: A review. Remote Sens. Appl. https://doi.org/10.1016/j.rsase.2023.101093.
Khan, W.R., Nazre, M., Akram, S., Anees, S.A., Mehmood, K., Ibrahim, F.H., Edrus, S.S.O. Al, Latiff, A., Fitri, Z.A., Yaseen, M., Li, P., Zhu, X., 2024. Assessing the productivity of the matang mangrove forest reserve: review of one of the best-managed mangrove forests. Forests. 15, 747. https://doi.org/10.3390/f15050747.
Khan, W.R., Rasheed, F., Zulkifli, S.Z., Kasim, M.R.B.M., Zimmer, M., Pazi, A.M., Kamrudin, N.A., Zafar, Z., Faridah-Hanum, I., Nazre, M., 2020. Phytoextraction potential of Rhizophora apiculata: A case study in Matang mangrove forest reserve. Malaysia. Trop. Conser. Sci. 13, 1940082920947344.
Khaniya, B., Priyantha, H.G., Baduge, N., Azamathulla, H.M., Rathnayake, U., 2020. Impact of climate variability on hydropower generation: A case study from Sri Lanka. ISH J. Hydraulic Eng. 26 https://doi.org/10.1080/09715010.2018.1485516.
Kunert, N., Aparecido, L.M.T., 2024. Ecosystem carbon fluxes are tree size-dependent in an Amazonian old-growth forest. Agric. For. Meteorol. 346 https://doi.org/10.1016/j.agrformet.2024.109895.
Li, C., Wang, Y., Wu, X., Cao, H., Li, W., Wu, T., 2021. Reducing human activity promotes environmental restoration in arid and semi-arid regions: A case study in Northwest China. Sci. Total Environ. 768 https://doi.org/10.1016/j.scitotenv.2020.144525.
Li, H., Zhang, H., Li, Q., Zhao, J., Guo, X., Ying, H., Deng, G., Rihan, W., Wang, S., 2021. Vegetation productivity dynamics in response to climate change and human activities under different topography and land cover in northeast china. Remote Sens. (Basel) 13. https://doi.org/10.3390/rs13050975.
Li, Y., Li, L., Dong, J., Bai, J., 2021. Assessing MODIS carbon and water fluxes in grasslands and shrublands in semiarid regions using eddy covariance tower data. Int. J. Remote Sens. 42 https://doi.org/10.1080/01431161.2020.1811915.
Li, Z., Jiao, Z., Wang, C., Yin, S., Guo, J., Tong, Y., Gao, G., Tan, Z., Chen, S., 2023. Seasonal effect of the vegetation clumping index on gross primary productivity estimated by a two-leaf light use efficiency model. Remote Sens. (Basel) 15. https://doi.org/10.3390/rs15235537.
Lian, X., Jiao, L., Liu, Z., 2023. Saturation response of enhanced vegetation productivity attributes to intricate interactions. Glob. Chang. Biol. 29 https://doi.org/10.1111/gcb.16522.
Liao, Z., Zhou, B., Zhu, J., Jia, H., Fei, X., 2023. A critical review of methods, principles and progress for estimating the gross primary productivity of terrestrial ecosystems. Front. Environ. Sci. https://doi.org/10.3389/fenvs.2023.1093095.
Liu, M., Chen, Yinrong, Chen, K., Chen, Yi, 2023. Progress and hotspots of research on land-use carbon emissions: a global perspective. Sustainability (Switzerland). https://doi.org/10.3390/su15097245.
Liu, Z., Wang, H., Li, N., Zhu, J., Pan, Z., Qin, F., 2020. Spatial and temporal characteristics and driving forces of vegetation changes in the huaihe river basin from 2003 to 2018. Sustainability (Switzerland) 12. https://doi.org/10.3390/su12062198.
Liu, Z., Wang, L., Wang, S., 2014. Comparison of different GPP models in China using MODIS image and ChinaFLUX data. Remote Sens. (Basel) 6. https://doi.org/10.3390/rs61010215.
Liu, Z., Wang, W., Chen, Y., Wang, L., Guo, Z., Yang, X., Yan, J., 2023. Solar harvest: Enhancing carbon sequestration and energy efficiency in solar greenhouses with PVT and GSHP systems. Renew. Energy 211. https://doi.org/10.1016/j.renene.2023.04.133.
Long, Q., Wang, F., Ge, W., Jiao, F., Han, J., Chen, H., Roig, F.A., Abraham, E.M., Xie, M., Cai, L., 2023. Temporal and spatial change in vegetation and its interaction with climate change in Argentina from 1982 to 2015. Remote Sens. (Basel) 15. https://doi.org/10.3390/rs15071926.

Lu, Z., Chen, P., Yang, Y., Zhang, S., Zhang, C., Zhu, H., 2023. Exploring quantification and analyzing driving force for spatial and temporal differentiation characteristics of vegetation net primary productivity in Shandong Province. China. Ecol. Indic. 153 https://doi.org/10.1016/j.ecolind.2023.110471.

Luo, M., Anees, S.A., Huang, Q., Qin, X., Qin, Z., Fan, J., Han, G., Zhang, L., Shafri, H.Z. M., 2024. Improving forest above-ground biomass estimation by integrating individual machine learning models. Forests. 15 (6), 975. https://doi.org/10.3390/f15060975.

Luo, X., Wang, Y., Li, Y., 2023. Responses of ecosystem water use efficiency to drought in the Lancang–Mekong River Basin. Front. Ecol. Evol. 11 https://doi.org/10.3389/fevo.2023.1203725.

Lv, Y., Liu, J., He, W., Zhou, Y., Tu Nguyen, N., Bi, W., Wei, X., Chen, H., 2023. How well do light-use efficiency models capture large-scale drought impacts on vegetation productivity compared with data-driven estimates? Ecol. Indic. 146 https://doi.org/10.1016/j.ecolind.2022.109739.

Lyu, J., Fu, X., Lu, C., Zhang, Y., Luo, P., Guo, P., Huo, A., Zhou, M., 2023. Quantitative assessment of spatiotemporal dynamics in vegetation NPP, NEP and carbon sink capacity in the Weihe River Basin from 2001 to 2020. J. Clean. Prod. 428 https://doi.org/10.1016/j.jclepro.2023.139384.

Manzoni, S., Taylor, P., Richter, A., Porporato, A., Ågren, G.I., 2012. Environmental and stoichiometric controls on microbial carbon-use efficiency in soils. New Phytologist. https://doi.org/10.1111/j.1469-8137.2012.04225.x.

Martin-Benito, D., Molina-Valero, J.A., Pérez-Cruzado, C., Bigler, C., Bugmann, H., 2022. Development and long-term dynamics of old-growth beech-fir forests in the Pyrenees: Evidence from dendroecology and dynamic vegetation modelling. For. Ecol. Manage 524. https://doi.org/10.1016/j.foreco.2022.120541.

Mashao, F.M., Mothapo, M.C., Munyai, R.B., Letsoalo, J.M., Mbokodo, I.L., Muofhe, T.P., Matsane, W., Chikoore, H., 2023. Extreme rainfall and flood risk prediction over the east coast of South Africa. Water (Switzerland) 15. https://doi.org/10.3390/w15010050.

Massey, R., Berner, L.T., Foster, A.C., Goetz, S.J., Vepakomma, U., 2023. Remote Sensing tools for monitoring forests and tracking their dynamics. Advances in Global Change Research. https://doi.org/10.1007/978-3-031-15988-6_26.

Mazlan, S.M., Jaafar, W.S.W.M., Kamarulzaman, A.M.M., Saad, S.N.M., Ghazali, N.M., Adrah, E., Maulud, K.N.A., Omar, H., Teh, Y.A., Dzulkifli, D., Mahmud, M.R., 2023. A Review on the Use of LiDAR Remote Sensing for Forest Landscape Restoration, in: Concepts and Applications of Remote Sensing in Forestry. https://doi.org/10.1007/978-981-19-4200-6_3.

Mehmood, K., Anees, S.A., Luo, M., Akram, M., Zubair, M., Khan, K.A., Khan, W.R., 2024a. Assessing chilgoza pine (pinus gerardiana) forest fire severity: remote sensing analysis, correlations, and predictive modeling for enhanced management strategies. Trees. For. People, 100521. https://doi.org/10.1016/j.tfp.2024.100521.

Mehmood, K., Anees, S.A., Muhammad, S., Hussain, K., Shahzad, F., Liu, Q., Ansari, M.J., Alharbi, S.A., Khan, W.R., 2024b. Analyzing vegetation health dynamics across seasons and regions through NDVI and climatic variables. Sci. Rep. 14 (1), 11775. https://doi.org/10.1038/s41598-024-62464-7.

Mehmood, K., Anees, S.A., Rehman, A., Tariq, A., Liu, Q., Muhammad, S., Rabbi, F., Pan, S.A., Hatamleh, W.A., 2024c. Assessing forest cover changes and fragmentation in the Himalayan Temperate Region: Implications for forest conservation and management. J. For. Res. (Harbin) 35 (1), 82. https://doi.org/10.1007/s11676-024-01734-6.

Mehmood, K., Anees, S.A., Rehman, A., Tariq, A., Zubair, M., Liu, Q., Rabbi, F., Khan, K. A., Luo, M., 2024d. Exploring spatiotemporal dynamics of NDVI and climate-driven responses in ecosystems: Insights for sustainable management and climate resilience. Ecol. Inform., 102532 https://doi.org/10.1016/j.ecoinf.2024.102532.

Milesi, C., Kukunuri, M., 2022. Crop yield estimation at gram panchayat scale by integrating field, weather and satellite data with crop simulation models. J. Indian Soc. Remote Sens. 50 https://doi.org/10.1007/s12524-021-01372-z.

Miranda, J.C., Calderaro, C., Cocozza, C., Lasserre, B., Tognetti, R., von Arx, G., 2022. Wood anatomical responses of european beech to elevation, land use change, and climate variability in the central apennines. Italy. Front Plant Sci 13. https://doi.org/10.3389/fpls.2022.855741.

Mohammadi, M., Sharifi, A., 2021. Evaluation of convolutional neural networks for urban mapping using satellite images. J. Indian Society of. Remote Sens. 49 (9), 2125–2131.

Muhammad, S., Hamza, A., Mehmood, K., Adnan, M., Tayyab, M., 2023. Analyzing the impact of forest harvesting ban in northern temperate forest. A case study of Anakar Valley, Kalam Swat Region, Khyber-Pakhtunkhwa, Pakistan. Pure Appl. Biol. 12 (2), 1434–1439.

Muñoz Sabater, J., 2019. ERA5-land monthly averaged data from 1981 to present, Copernicus Climate Change Service (C3S) Climate Data Store (CDS). Earth Syst. Sci. Data 55, 5679–5695.

Muñoz-Sabater, J., Dutra, E., Agustí-Panareda, A., Albergel, C., Arduini, G., Balsamo, G., Boussetta, S., Choulga, M., Harrigan, S., Hersbach, H., Martens, B., Miralles, D.G., Piles, M., Rodríguez-Fernández, N.J., Zsoter, E., Buontempo, C., Thépaut, J.-N., 2021a. ERA5-Land: a state-of-the-art global reanalysis dataset for land applications. Earth. Syst. Sci. Data 13, 4349–4383. https://doi.org/10.5194/essd-13-4349-2021.

Muñoz-Sabater, J., Dutra, E., Agustí-Panareda, A., Albergel, C., Arduini, G., Balsamo, G., Boussetta, S., Choulga, M., Harrigan, S., Hersbach, H., Martens, B., Miralles, D.G., Piles, M., Rodríguez-Fernández, N.J., Zsoter, E., Buontempo, C., Thépaut, J.-N., 2021b. ERA5-Land: a state-of-the-art global reanalysis dataset for land applications. Earth. Syst. Sci. Data 13, 4349–4383. https://doi.org/10.5194/essd-13-4349-2021.

Naghdizadegan Jahromi, M., Naghdyzadegan Jahromi, M., Pourghasemi, H.R., Zand-Parsa, S., Jamshidi, S., 2021. Accuracy assessment of forest mapping in MODIS land cover dataset using fuzzy set theory. Forest Resources Resilience and Conflicts. https://doi.org/10.1016/B978-0-12-822931-6.00012-5.

Nejad, S.M.M., Abbasi-Moghadam, D., Sharifi, A., Farmonov, N., Amankulova, K., László, M., 2022. Multispectral crop yield prediction using 3D-convolutional neural networks and attention convolutional LSTM approaches. IEEE J. Sel. Top. Appl. Earth. Obs. Remote Sens. 16, 254–266.

Nouvellon, Y., Seen, D.Lo, Rambal, S., Bégué, A., Moran, M.S., Kerr, Y., Qi, J., 2000. Time course of radiation use efficiency in a shortgrass ecosystem: Consequences for remotely sensed estimation of primary production. Remote Sens. Environ. 71 https://doi.org/10.1016/S0034-4257(99)00063-2.

Nyikadzino, B., Chitakira, M., Muchuru, S., 2020. Rainfall and runoff trend analysis in the Limpopo river basin using the Mann Kendall statistic. Phys. Chem. Earth 117. https://doi.org/10.1016/j.pce.2020.102870.

Pan, S.A., Anees, S.A., Li, X., Yang, X., Duan, X., Li, Z., 2023. Spatial and Temporal patterns of non-structural carbohydrates in faxon fir (abies fargesii var. faxoniana), subalpine mountains of southwest China. Forests. 14 (7), 1438. https://doi.org/10.3390/f14071438.

Patacca, M., Lindner, M., Lucas-Borja, M.E., Cordonnier, T., Fidej, G., Gardiner, B., Hauf, Y., Jasinevičius, G., Labonne, S., Linkevičius, E., Mahnken, M., Milanovic, S., Nabuurs, G.J., Nagel, T.A., Nikinmaa, L., Panyatov, M., Bercak, R., Seidl, R., Ostrogović Sever, M.Z., Socha, J., Thom, D., Vuletic, D., Zudin, S., Schelhaas, M.J., 2023. Significant increase in natural disturbance impacts on European forests since 1950. Glob. Chang. Biol. 29 https://doi.org/10.1111/gcb.16531.

Perez-Quezada, J.F., Barichivich, J., Urrutia-Jalabert, R., Carrasco, E., Aguilera, D., Bacour, C., Lara, A., 2023. Warming and drought weaken the carbon sink capacity of an endangered paleoendemic temperate rainforest in South America. J. Geophys. Res. Biogeosci. 128 https://doi.org/10.1029/2022JG007258.

Piton, G., Legay, N., Arnoldi, C., Lavorel, S., Clément, J.C., Foulquier, A., 2020. Using proxies of microbial community-weighted means traits to explain the cascading effect of management intensity, soil and plant traits on ecosystem resilience in mountain grasslands. J. Ecol. 108 https://doi.org/10.1111/1365-2745.13327.

Polley, H.W., Isbell, F.I., Wilsey, B.J., 2013. Plant functional traits improve diversity-based predictions of temporal stability of grassland productivity. Oikos. 122 https://doi.org/10.1111/j.1600-0706.2013.00338.x.

Qin, J., Ma, M., Zhu, Y., Wu, B., Su, X., 2023. 3PG-MT-LSTM: A Hybrid Model under biomass compatibility constraints for the prediction of long-term forest growth to support sustainable management. Forests. 14 https://doi.org/10.3390/f14071482.

Qiu, Y., Zhang, L., Fan, D., 2018. Spatio-temporal changes of net primary productivity and its response to phenology in northeast China during 2000-2015. International Archives of the Photogrammetry, Remote Sensing and Spatial Information Sciences - ISPRS Archives. https://doi.org/10.5194/isprs-archives-XLII-3-1453-2018.

Quinkenstein, A., Tsonkova, P., Freese, D., 2018. Alley cropping with short rotation coppices in the temperate region: A land-use strategy for optimizing microclimate, soil organic carbon and ecosystem service provision of agricultural landscapes. Agroforestry: Anecdotal to Modern Science. https://doi.org/10.1007/978-981-10-7650-3_10.

Raich, J.W., Russell, A.E., Vitousek, P.M., 1997. Primary productivity and ecosystem development along an elevational gradient on Mauna Loa, Hawai'i. Ecology. 78 https://doi.org/10.1890/0012-9658(1997)078[0707:PPAEDA]2.0.CO;2.

Ramirez, E., 2016. U.S. Releases Enhanced Shuttle Land Elevation Data. Nasa.

Rana, B.S., Singh, S.P., Singh, R.P., 1989. Biomass and net primary productivity in Central Himalayan forests along an altitudinal gradient. For. Ecol. Manage 27. https://doi.org/10.1016/0378-1127(89)90107-2.

Raza, A., Charagh, S., Abbas, S., Hassan, M.U., Saeed, F., Haider, S., Sharif, R., Anand, A., Corpas, F.J., Jin, W., Varshney, R.K., 2023. Assessment of proline function in higher plants under extreme temperatures. Plant Biol. https://doi.org/10.1111/plb.13510.

Ren, Z., Qiao, H., Xiong, P., Peng, J., Wang, B., Wang, K., 2023. Characteristics and driving factors of precipitation-use efficiency across diverse grasslands in chinese loess plateau. Agronomy 13. https://doi.org/10.3390/agronomy13092296.

Rita, A., Camarero, J.J., Nolè, A., Borghetti, M., Brunetti, M., Pergola, N., Serio, C., Vicente-Serrano, S.M., Tramutoli, V., Ripullone, F., 2020. The impact of drought spells on forests depends on site conditions: The case of 2017 summer heat wave in southern Europe. Glob. Chang. Biol. 26 https://doi.org/10.1111/gcb.14825.

Running, S., Zhao, M., 2019. MOD17A3HGF MODIS/Terra Net Primary Production Gap-Filled Yearly L4 Global 500 m SIN Grid V006 [WWW Document]. NASA EOSDIS Land Processes DAAC.

Sa, R., Fan, W., 2023. Estimation of forest parameters in boreal artificial coniferous forests using landsat 8 and sentinel-2A. Remote Sens. (Basel) 15, 3605.

Sabzchi-Dehkharghani, H., Biswas, A., Meshram, S.G., Majnooni-Heris, A., 2024. Estimating gross and net primary productivities using earth observation products: a review. Environ. Model. Assess. (Dordr). https://doi.org/10.1007/s10666-023-09927-9.

Sayed, S.A., González, P.A., 2014. Flood disaster profile of Pakistan: A review. Sci. J. Public Health 2, 144–149.

Schwartz, M.W., Butt, N., Dolanc, C.R., Holguin, A., Moritz, M.A., North, M.P., Safford, H.D., Stephenson, N.L., Thorne, J.H., van Mantgem, P.J., 2015. Increasing elevation of fire in the Sierra Nevada and implications for forest change. Ecosphere 6, 1–10.

Shafeeque, M., Sarwar, A., Basit, A., Mohamed, A.Z., Rasheed, M.W., Khan, M.U., Buttar, N.A., Saddique, N., Asim, M.I., Sabir, R.M., 2022. Quantifying the impact of the billion tree afforestation project (BTAP) on the water yield and sediment load in the tarbela reservoir of Pakistan using the SWAT model. Land. (Basel) 11. https://doi.org/10.3390/land11101650.

Shahzad, F., Mehmood, K., Hussain, K., Haidar, I., Anees, S.A., Muhammad, S., Ali, J., Adnan, M., Wang, Z., Feng, Z., 2024. Comparing machine learning algorithms to predict vegetation fire detections in Pakistan. Fire Ecol. 20 (1), 1–20. https://doi.org/10.1186/s42408-024-00289-5.

Sharifi, A., Hosseingholizadeh, M., 2020. Application of sentinel-1 data to estimate height and biomass of rice crop in Astaneh-ye Ashrafiyeh, Iran. J. Indian Soc. Remote Sens. 48, 11–19.
Sharifi, A., Felegari, S., 2022. Nitrogen dioxide (NO2) pollution monitoring with sentinel-5P satellite imagery over during the coronavirus pandemic (case study: Tehran). Remote Sens. Letter. 13 (10), 1029–1039.
Shi, X., Shi, M., Zhang, N., Wu, M., Ding, H., Li, Y., Chen, F., 2023. Effects of climate change and human activities on gross primary productivity in the Heihe River Basin. China. Environ. Sci. Pollut. Res. 30 https://doi.org/10.1007/s11356-022-22505-y.
Shobairi, S.O.R., Lin, H., Usoltsev, V.A., Osmirko, A.A., Tsepordey, I.S., Ye, Z., Anees, S. A., 2022. A comparative pattern for populus spp. and betula spp. stand biomass in eurasian climate gradients. Croatian J. Forest Eng.: J. Theory Appl. Forestry Eng. 43 (2), 457–467. https://doi.org/10.5552/crojfe.2022.1340.
Snyder, K.A., Richardson, W., Browning, D.M., Lieurance, W., Stringham, T.K., 2023. Plant phenology of high-elevation meadows: assessing spectral responses of grazed meadows. Rangel. Ecol. Manage 87. https://doi.org/10.1016/j.rama.2022.12.001.
Sobrino, J.A., Jiménez-Muñoz, J.C., 2014. Minimum configuration of thermal infrared bands for land surface temperature and emissivity estimation in the context of potential future missions. Remote Sens. Environ. 148, 158–167.
Society, T.E., Hu, Y., Yue, S., Wang, C.Y., Jain, S.K., Kumar, V., Rana, A., Uvo, C.B., Bengtsson, L., Sarthi, P.P., Yue, S., Pilon, P., Phinney, B., Cavadias, G., Biswas, B., Jadhav, R.S., Tikone, N., Gadedjisso-Tossou, A., Adjegan, K.I., Kablan, A.K.M., Janni, W., Nitz, U., Rack, B.K., Gluz, O., Schneeweiss, A., Kates, R.E., Fehm, T.N., Kreipe, H.H., Kummel, S., Wuerstlein, R., Hartkopf, A.D., Clemens, M., Reimer, T., Friedl, T.W.P., Haeberle, L., Fasching, P.A., Harbeck, N., Mondal, A., Kundu, S., Mukhopadhyay, A., Meshram, S.G., Singh, V.P., Meshram, C., Society, T.E., Hu, Y., Yue, S., Wang, C.Y., Caloiero, T., Coscarelli, R., Pellicone, G., Jain, S.K., Kumar, V., Subash, N., Sikka, A.K., Rana, A., Uvo, C.B., Bengtsson, L., Sarthi, P.P., Yue, S., Pilon, P., Phinney, B., Cavadias, G., Singh, R., Sah, S., Das, B., Vishnoi, L., Pathak, H., Ahmad, I., Zhang, F., Tayyab, M., Anjum, M.N., Zaman, M., Liu, J., Farid, H.U., Saddique, Q., Malik, A., Kumar, A., Guhathakurta, P., Kisi, O., Biswas, B., Jadhav, R. S., Tikone, N., Gadedjisso-Tossou, A., Adjegan, K.I., Kablan, A.K.M., Mondal, A., Kundu, S., Mukhopadhyay, A., Meshram, S.G., Singh, V.P., Meshram, C., Singh, R., Sah, S., Das, B., Potekar, S., Chaudhary, A., Pathak, H., Marak, J.D.K., Sarma, A.K., Bhattacharjya, R.K., Arab Amiri, M., Gocić, M., Wang, Y., Xu, Y., Tabari, H., Wang, J., Wang, Q., Song, S., Hu, Z., Cui, L., Wang, L., Lai, Z., Tian, Q., Liu, W., Li, J., Sen, Z., Malik, A., Kumar, A., Pham, Q.B., Zhu, S., Linh, N.T.T., Tri, D.Q., IPCC, Caloiero, T., Sen, P.K., Cengiz, T.M., Tabari, H., Onyutha, C., Kisi, O., Caloiero, T., Coscarelli, R., Ferrari, E., Hare, W., Jain, S.K., Kumar, V., Saharia, M., Jain, S.K., Singh, Y., Kisi, O., Zerouali, B.B., Al-Ansari, N., Chettih, M., Mohamed, M., Abda, Z., Santos, C.A.G., Zerouali, B.B., Elbeltagi, A., Hamed, K., Rao, A.R., Radhakrishnan, K., Sivaraman, I., Jena, S.K., Sarkar, S., Adhikari, S., Pai, D.S., Sridhar, L., Rajeevan, M., Sreejith, O.P., Satbhai, N.S., Mukhopadhyay, B., Sen, Cengiz, T.M., Tabari, H., Onyutha, C., Kisi, O., Caloiero, T., Coscarelli, R., Ferrari, E., Jain, S.K., Kumar, V., Saharia, M., Jain, S.K., Singh, Y., Kisi, O., Theil, H., Pai, D.S., Sridhar, L., Rajeevan, M., Sreejith, O.P., Satbhai, N.S, Mukhopadhyay, B., Ahmad, I., Zhang, F., Tayyab, M., Anjum, M.N., Zaman, M., Liu, J., Farid, H.U., Saddique, Q., Arab Amiri, M., Gocić, M., Bisht, D.S., Chatterjee, C., Raghuwanshi, N.S., Sridhar, V., Biswas, B., Jadhav, R.S., Tikone, N., Caloiero, T., Coscarelli, R., Pellicone, G., Cui, L., Wang, L., Lai, Z., Tian, Q., Liu, W., Li, J., Gadedjisso-Tossou, A., Adjegan, K.I., Kablan, A.K.M., Gajbhiye, S., Meshram, C., Mirabbasi, R., Sharma, S.K., Jain, S.K., Kumar, V., Saharia, M., Janni, W., Nitz, U., Rack, B.K., Gluz, O., Schneeweiss, A., Kates, R.E., Fehm, T.N., Kreipe, H.H., Kummel, S., Wuerstlein, R., Hartkopf, A.D., Clemens, M., Reimer, T., Friedl, T.W.P., Haeberle, L., Fasching, P.A., Harbeck, N., Kumar, V., Jain, S.K., Singh, Y., Malik, A., Kumar, A., Guhathakurta, P., Kisi, O., Pham, Q.B., Zhu, S., Linh, N.T.T., Tri, D.Q., Marak, J.D.K., Sarma, A.K., Bhattacharjya, R.K., Meshram, S.G., Singh, V.P., Meshram, C., Mondal, A., Khare, D., Kundu, S., Mukhopadhyay, A., Radhakrishnan, K., Sivaraman, I., Jena, S.K., Sarkar, S., Adhikari, S., Rana, A., Uvo, C.B., Bengtsson, L., Sarthi, P.P., Singh, R., Sah, S., Das, B., Potekar, S., Chaudhary, A., Pathak, H., Vishnoi, L., Pathak, H., Society, T.E., Hu, Y., Yue, S., Wang, C.Y., Subash, N., Sikka, A.K., Wang, Y., Xu, Y., Tabari, H., Wang, J., Wang, Q., Song, S., Hu, Z., Gajbhiye, S., Meshram, C., Mirabbasi, R., Sharma, S.K., Malik, A., Kumar, A., Guhathakurta, P., Kisi, O., 2021. A rank-invariant method for linear and polynomial regression. Theor. Appl. Climatol.
Song, X., Mi, N., Mi, W., Li, L., 2022. Spatial non-stationary characteristics between grass yield and its influencing factors in the Ningxia temperate grasslands based on a mixed geographically weighted regression model. J. Geograph. Sci. 32 https://doi.org/10.1007/s11442-022-1986-5.
Takaku, J., Tadono, T., Doutsu, M., Ohgushi, F., Kai, H., 2020. Updates of aw3d30' alos global digital surface model with other open access datasets, in: International Archives of the Photogrammetry, Remote Sensing and Spatial Information Sciences - ISPRS Archives. https://doi.org/10.5194/isprs-archives-XLIII-B4-2020-183-2020.
Tao, J., Xie, Y., Wang, W., Zhu, J., Zhang, Y., Zhang, X., 2022. Elevational gradient of climate-driving effects on cropland ecosystem net primary productivity in alpine region of the southwest China. Remote Sens. (Basel) 14. https://doi.org/10.3390/rs14133069.
Teng, H., Chen, S., Hu, B., Shi, Z., 2023. Future changes and driving factors of global peak vegetation growth based on CMIP6 simulations. Ecol. Inform. 75 https://doi.org/10.1016/j.ecoinf.2023.102031.
Teng, M., Zeng, L., Hu, W., Wang, P., Yan, Z., He, W., Zhang, Y., Huang, Z., Xiao, W., 2020. The impacts of climate changes and human activities on net primary productivity vary across an ecotone zone in Northwest China. Sci. Total Environ. 714 https://doi.org/10.1016/j.scitotenv.2020.136691.
Teubner, I.E., Forkel, M., Camps-Valls, G., Jung, M., Miralles, D.G., Tramontana, G., van der Schalie, R., Vreugdenhil, M., Mösinger, L., Dorigo, W.A., 2019. A carbon sink-driven approach to estimate gross primary production from microwave satellite observations. Remote Sens. Environ. 229 https://doi.org/10.1016/j.rse.2019.04.022.
Tu, H., Jiapaer, G., Yu, T., Li, X., Chen, B., 2023. Analysis of spatio-temporal variation characteristics and influencing factors of net primary productivity in terrestrial ecosystems of China. Shengtai Xuebao 43. https://doi.org/10.5846/stxb202201230216.
Ukkola, A.M., De Kauwe, M.G., Roderick, M.L., Burrell, A., Lehmann, P., Pitman, A.J., 2021. Annual precipitation explains variability in dryland vegetation greenness globally but not locally. Glob. Chang. Biol. 27, 4367–4380.
Ullah, I., Saleem, A., Ansari, L., Ali, N., Ahmad, N., Dar, N.M., Din, N.U., 2020. Growth and survival of multipurpose species; assessing billion tree afforestation project (BTAP), the bonn challenge initiative. Appl. Ecol. Environ. Res. 18 https://doi.org/10.15666/aeer/1802_20572072.
Usoltsev, V.A., Chen, B., Shobairi, S.O.R., Tsepordey, I.S., Chasovskikh, V.P., Anees, S.A., 2020. Patterns for Populus spp. stand biomass in gradients of winter temperature and precipitation of. Eurasia. Forests 11 (9), 906. https://doi.org/10.3390/f11090906.
Usoltsev, V.A., Lin, H., Shobairi, S.O.R., Tsepordey, I.S., Ye, Z., Anees, S.A., 2022. The principle of space-for-time substitution in predicting Betula spp. Biomass change related to climate shifts. Appl. Ecol. Environ. Res. 20 (4), 3683–3698. https://doi.org/10.15666/aeer/2004_36833698.
Vacek, Z., Vacek, S., Cukor, J., 2023. European forests under global climate change: Review of tree growth processes, crises and management strategies. J. Environ. Manage. https://doi.org/10.1016/j.jenvman.2023.117353.
Vargas Godoy, M.R., Markonis, Y., 2023. pRecipe: A global precipitation climatology toolbox and database. Environmental Modelling and Software 165. https://doi.org/10.1016/j.envsoft.2023.105711.
Verma, Mani Kant, Verma, M.K., Swain, S., 2016. Statistical analysis of precipitation over Seonath River Basin, Chhattisgarh, India. Int. J. Appl. Eng. Res. 11.
Wang, C., Yu, W., Ma, L., Ye, X., Erdenebileg, E., Wang, R., Huang, Z., Indree, T., Liu, G., 2023. Biotic and abiotic drivers of ecosystem multifunctionality: Evidence from the semi-arid grasslands of northern China. Sci. Total Environ. 887 https://doi.org/10.1016/j.scitotenv.2023.164158.
Wang, D., Liang, S., Zhang, Y., Gao, X., Brown, M.G.L., Jia, A., 2020. A new set of modis land products (Mcd18): Downward shortwave radiation and photosynthetically active radiation. Remote Sens. (Basel) 12. https://doi.org/10.3390/RS12010168.
Wang, J., Zhen, J., Hu, W., Chen, S., Lizaga, I., Zeraatpisheh, M., Yang, X., 2023. Remote sensing of soil degradation: Progress and perspective. Int. Soil Water Conser. Res. https://doi.org/10.1016/j.iswcr.2023.03.002.
Wang, T., Yang, M., Yan, S., Geng, G., Li, Q., Wang, F., 2021. Effects of temperature and precipitation on spatiotemporal variations of net primary productivity in the Qinling Mountains. China. Pol J Environ Stud 30. https://doi.org/10.15244/pjoes/122839.
Wang, Y.-R., Hessen, D.O., Samset, B.H., Stordal, F., 2022. Evaluating global and regional land warming trends in the past decades with both MODIS and ERA5-Land land surface temperature data. Remote Sens. Environ. 280, 113181.
Wang, Z., Wang, H., Wang, T., Wang, L., Huang, X., Zheng, K., Liu, X., 2022. Effects of environmental factors on the changes in MODIS NPP along DEM in global terrestrial ecosystems over the last two decades. Remote Sens. (Basel) 14. https://doi.org/10.3390/rs14030713.
Wani, O.A., Sharma, V., Kumar, S.S., Babu, S., Sharma, K.R., Rathore, S.S., Marwaha, S., Ganai, N.A., Dar, S.R., Yeasin, M., Singh, R., Tomar, J., 2023. Climate plays a dominant role over land management in governing soil carbon dynamics in North Western Himalayas. J. Environ. Manage 338. https://doi.org/10.1016/j.jenvman.2023.117740.
Wei, C., Zeng, J., Wang, J., Jiang, X., You, Y., Wang, L., Zhang, Y., Liao, Z., Su, K., 2023. Assessing the impact of climate and human activities on ecosystem services in the loess plateau ecological screen. China. Remote Sens (Basel) 15. https://doi.org/10.3390/rs15194717.
Wiltshire, A.J., Burke, E.J., Chadburn, S.E., Jones, C.D., Cox, P.M., Davies-Barnard, T., Friedlingstein, P., Harper, A.B., Liddicoat, S., Sitch, S., Zaehle, S., 2021. Jules-cn: A coupled terrestrial carbon-nitrogen scheme (jules vn5.1). Geosci. Model. Dev. 14 https://doi.org/10.5194/gmd-14-2161-2021.
Wongnakae, P., Chitchum, P., Sripramong, R., Phosri, A., 2023. Application of satellite remote sensing data and random forest approach to estimate ground-level PM2.5 concentration in Northern region of Thailand. Environ. Sci. Pollut. Res. 30 https://doi.org/10.1007/s11356-023-28698-0.
Xi, X., Yuan, X., 2023. Remote sensing of atmospheric and soil water stress on ecosystem carbon and water use during flash droughts over eastern China. Sci. Total Environ. 868 https://doi.org/10.1016/j.scitotenv.2023.161715.
Xu, B., Feng, Z., Chen, Y., Zhou, Y., Shao, Y., Wang, Z., 2024. Assessing the distribution and driving effects of net primary productivity along an elevation gradient in subtropical regions of China. Forests. 15 https://doi.org/10.3390/f15020340.
Xu, J., Badola, R., Chettri, N., Chaudhary, R.P., Zomer, R., Pokhrel, B., Hussain, S.A., Pradhan, S., Pradhan, R., 2019. Sustaining biodiversity and ecosystem services in the hindu Kush Himalaya. In: Wester, P., Mishra, A., Mukherji, A., Shrestha, A.B. (Eds.), The Hindu Kush Himalaya Assessment: Mountains, Climate Change, Sustainability and People. Springer International Publishing, Cham, pp. 127–165. https://doi.org/10.1007/978-3-319-92288-1_5.
Xue, S., Ma, B., Wang, C., Li, Z., 2023. Identifying key landscape pattern indices influencing the NPP: A case study of the upper and middle reaches of the Yellow River. Ecol. Modell. 484 https://doi.org/10.1016/j.ecolmodel.2023.110457.
Yan, Y., Xu, X., Liu, X., Wen, Y., Ou, J., 2020. Assessing the contributions of climate change and human activities to cropland productivity by means of remote sensing. Int. J. Remote Sens. 41 https://doi.org/10.1080/01431161.2019.1681603.

Yang, Ziyan, Yu, Q., Yang, Ziyu, Peng, A., Zeng, Y., Liu, W., Zhao, J., Yang, D., 2023. Spatio-temporal dynamic characteristics of carbon use efficiency in a virgin forest area of southeast tibet. Remote Sens. (Basel) 15. https://doi.org/10.3390/rs15092382.

Yin, C., Chen, X., Luo, M., Meng, F., Sa, C., Bao, S., Yuan, Z., Zhang, X., Bao, Y., 2023. Quantifying the contribution of driving factors on distribution and change of net primary productivity of vegetation in the mongolian plateau. Remote Sens. (Basel) 15. https://doi.org/10.3390/rs15081986.

Yin, C., Luo, M., Meng, F., Sa, C., Yuan, Z., Bao, Y., 2022. Contributions of climatic and anthropogenic drivers to net primary productivity of vegetation in the mongolian plateau. Remote Sens. (Basel) 14. https://doi.org/10.3390/rs14143383.

Yu, P., Zhang, Y., Liu, P., Zhang, Jinsong, Xing, W., Tong, X., Zhang, Jingru, Meng, P., 2024. Regulation of biophysical drivers on carbon and water fluxes over a warm-temperate plantation in northern China. Sci. Total Environ. 907 https://doi.org/10.1016/j.scitotenv.2023.167408.

Yuan, W., Chen, Y., Xia, J., Dong, W., Magliulo, V., Moors, E., Olesen, J.E., Zhang, H., 2015. Estimating crop yield using a satellite-based light use efficiency model. Ecol. Indic. 60 https://doi.org/10.1016/j.ecolind.2015.08.013.

Yuan, W., Liu, S., Yu, G., Bonnefond, J.M., Chen, J., Davis, K., Desai, A.R., Goldstein, A. H., Gianelle, D., Rossi, F., Suyker, A.E., Verma, S.B., 2010. Global estimates of evapotranspiration and gross primary production based on MODIS and global meteorology data. Remote Sens. Environ. 114 https://doi.org/10.1016/j.rse.2010.01.022.

Yuan, W., Liu, S., Zhou, Guangsheng, Zhou, Guoyi, Tieszen, L.L., Baldocchi, D., Bernhofer, C., Gholz, H., Goldstein, A.H., Goulden, M.L., Hollinger, D.Y., Hu, Y., Law, B.E., Stoy, P.C., Vesala, T., Wofsy, S.C., 2007. Deriving a light use efficiency model from eddy covariance flux data for predicting daily gross primary production across biomes. Agric. For. Meteorol. 143 https://doi.org/10.1016/j.agrformet.2006.12.001.

Zafar, Z., Mehmood, M.S., Ahamad, M.I., Chudhary, A., Abbas, N., Khan, A.R., Zulqarnain, R.M., Abdal, S., 2021. Trend analysis of the decadal variations of water bodies and land use/land cover through MODIS imagery: An in-depth study from Gilgit-Baltistan, Pakistan. Water. Sci. Technol. Water. Supply. 21 https://doi.org/10.2166/ws.2020.355.

Zhang, C., Zhen, H., Zhang, S., Tang, C., 2023. Dynamic changes in net primary productivity of marsh wetland vegetation in China from 2005 to 2015. Ecol. Indic. 155 https://doi.org/10.1016/j.ecolind.2023.110970.

Zhang, J., Wang, X., Ren, J., 2021. Simulation of gross primary productivity using multiple light use efficiency models. Land. (Basel) 10. https://doi.org/10.3390/land10030329.

Zhang, L.X., Zhou, D.C., Fan, J.W., Hu, Z.M., 2015. Comparison of four light use efficiency models for estimating terrestrial gross primary production. Ecol. Modell. 300 https://doi.org/10.1016/j.ecolmodel.2015.01.001.

Zhang, M., Li, J., Li, N., Sun, W., Li, P., Zhao, Y., 2024. Spatial inhomogeneity of synoptic-induced precipitation in a region of steep topographic relief: a case study. J. Geophys. Res.: Atmospheres 129. https://doi.org/10.1029/2023JD039129.

Zhang, W., Luo, G., Hamdi, R., Ma, X., Termonia, P., De Maeyer, P., 2024. Drought changes the dominant water stress on the grassland and forest production in the northern hemisphere. Agric. For. Meteorol. 345 https://doi.org/10.1016/j.agrformet.2023.109831.

Zhang, X., Wang, Y., Wang, J., Yu, M., Zhang, R., Mi, Y., Xu, J., Jiang, R., Gao, J., 2024. Elevation influences belowground biomass proportion in forests by affecting climatic factors, soil nutrients and key leaf traits. Plants 13. https://doi.org/10.3390/plants13050674.

Zhang, Y., Hu, Q., Zou, F., 2021. Spatio-temporal changes of vegetation net primary productivity and its driving factors on the Qinghai-Tibetan plateau from 2001 to 2017. Remote Sens. (Basel) 13. https://doi.org/10.3390/rs13081566.

Zhao, F., Zhang, S., Du, Q., Ding, J., Luan, G., Xie, Z., 2021. Assessment of the sustainable development of rural minority settlements based on multidimensional data and geographical detector method: A case study in Dehong, China. Socioecon. Plann. Sci. 78 https://doi.org/10.1016/j.seps.2021.101066.

Zhao, G., Liu, M., Shi, P., Zong, N., Wang, J., Wu, J., Zhang, X., 2019. Spatial-temporal variation of ANPP and rain-use efficiency along a precipitation gradient on Changtang Plateau. Tibet. Remote Sens (Basel) 11. https://doi.org/10.3390/rs11030325.

Zhao, J., Dong, Y., Zhang, M., Huang, L., 2020. Comparison of identifying land cover tempo-spatial changes using GlobCover and MCD12Q1 global land cover products. Arabian J.Geosci. 13 https://doi.org/10.1007/s12517-020-05780-2.

Zhou, B., Liao, Z., Chen, S., Jia, H., Zhu, J., Fei, X., 2022. Net primary productivity of forest ecosystems in the southwest karst region from the perspective of carbon neutralization. Forests. https://doi.org/10.3390/f13091367.

Zhou, X., Peng, B., Zhou, Y., Yu, F., Wang, X.C., 2022. Quantifying the influence of climate change and anthropogenic activities on the net primary productivity of china's grasslands. Remote Sens. (Basel) 14. https://doi.org/10.3390/rs14194844.

Zhou, Z., Ding, Y., Shi, H., Cai, H., Fu, Q., Liu, S., Li, T., 2020. Analysis and prediction of vegetation dynamic changes in China: Past, present and future. Ecol. Indic. 117, 106642.

Zianis, D., Mencuccini, M., 2005. Aboveground net primary productivity of a beech (Fagus moesiaca) forest: A case study of Naousa forest, northern Greece. Tree Physiol. 25 https://doi.org/10.1093/treephys/25.6.713.

Further reading

Xie, Z., Zhao, C., Zhu, W., Zhang, H., Fu, Y.H., 2023. A radiation-regulated dynamic maximum light use efficiency for improving gross primary productivity estimation. Remote Sens. (Basel) 15. https://doi.org/10.3390/rs15051176.